CHALMERS
UNIVERSITY OF TECHNOLOGY

Dynamic Study of LNG Fuel Gas Supply Systems

In cooperation with ÅF-Pöyry and MAN Energy Solutions

Master's thesis in Innovative and Sustainable Chemical Engineering

GUSTAV QUINT
MONICA BOTHA

Department of Space, Earth and Environment
CHALMERS UNIVERSITY OF TECHNOLOGY
Gothenburg, Sweden 2019

Master's thesis 2019

Dynamic Study of LNG Fuel Gas Supply System

In cooperation with ÅF-Pöyry and MAN Energy Solutions

GUSTAV QUINT
MONICA BOTHA

Department of Space, Earth and Environment
Division of Energy Technology
Chalmers University of Technology
Gothenburg, Sweden 2019

Dynamic Study of LNG Fuel Gas Supply System
In cooperation with ÅF-Pöyry and MAN Energy Solutions
GUSTAV QUINT
MONICA BOTHA

Supervisor: Tobias Petersson, ÅF-Pöyry
Examiner: Stavros Papadokonstantakis, Space, Earth and Environment

Master's Thesis 2019
Department of Space, Earth and Environment
Division of Energy Technology
Chalmers University of Technology
SE-412 96 Gothenburg
Telephone +46 31 772 1000

Typeset in LaTeX
Printed by Chalmers Reproservice
Gothenburg, Sweden 2019

Dynamic Study of LNG Fuel Gas Supply System
In cooperation with ÅF-Pöyry and MAN Energy Solutions
GUSTAV QUINT, MONICA BOTHA
Department of Space, Earth and Environment
Chalmers University of Technology

Abstract

Liquefied natural gas (LNG) is an alternative fuel which is gaining popularity in the marine sector due to tougher emission regulations coming into effect in the year 2020. Due to the increased demand of marine LNG fuel, new larger scale gas supply systems are being developed. In this report, dynamic simulations of two new marine LNG fuel gas supply systems have been developed in HYSYS to study the control, buffer capacity and characteristics of the new systems. The evaluation has mainly been made by simulating various critical scenarios, such as emergency loadup, emergency shutdown, compressor start and low operating pressure. A control strategy has been made for the pumps and the compressor but not for the minimum flow line. Findings from the simulations show that the control strategy is able to handle most system changes without disruptions to the engines. It was also observed that the use of a buffer vessel alleviated disturbances but it was not deemed to be a necessity in a well tuned system.

Keywords: LNG, dynamic, simulation, HYSYS, control.

Contents

Acknowledgements

A lot of people contributed to the completion of this master thesis. First and foremost, we would like to thank Therese Tillander, Tobias Petersson and Bo Palmströmer from ÅF-Pöyry and our examiner Stavros Papadokonstantakis for entrusting us with a research that allowed us to contribute to the development in the process industry. We would also like to thank the rest of the process staff from ÅF-Pöyry for their contributions. Furthermore, we would like to thank the co-operators from MAN Energy Solutions who contributed with technical know-how and process data.

Finally, we would like to show our appreciation to our direct supervisor Tobias Petersson for his technical guidance which has been invaluable.

Gustav Quint and Monica Botha, Gothenburg, May 2019

List of abbreviations

BOG	Boil-off gas
EGCS	Exhaust gas cleaning system
ESD	Emergency shutdown
FGSS	Fuel gas supply system
GNG	Gaseous natural gas
GVU	Gas valve unit
HFO	Heavy fuel oil
IMO	International Maritime Organization
LNG	Liquefied natural gas
MGO	Marine gas oil
NOx	Nitrogen oxides
NPSH_R	Net positive suction head required
PBU	Pressure build-up unit
PID	Proportional-integral-derivative
PR	Peng-Robinson
PRSV	Peng-Robinson-Styjek-Vera
PT	Pressure transmitter
PU	Polyurethane
SRK	Soave-Redlich-Kwong
SOx	Sulphur oxides
VAP	Vaporization unit
TCS	Tank Control Space

1. Introduction

In recent years, the use of liquefied natural gas (LNG) as a fuel in ships has become more popular as it produces significantly lower amounts of air pollutants such as SOx, NOx, particle matter and CO_2 than the conventional heavy fuel oil (HFO)[1]. In 2020 the emission regulation MARPOL Annex VI, which forbids ships to run on fuels with a sulfur content higher than 0.5% globally and 0.1% inside emission control areas, will come to effect [2]. Ships will then be prohibited from the conventional use of HFO and must change to one of three alternatives: a low sulfur fuel oil/diesel called maritime gas oil (MGO), LNG fuel or an exhaust gas cleaning system (EGCS) [3]. There are other solutions to lower the emissions such as methanol, ammonia, electric drive or similar [4, 5] but they can not be considered large scale alternatives in the near future.

Switching to MGO is the easiest alternative since it requires minimal changes to the fuel gas supply system and engines. MGO is however expensive and will probably increase even more in price as demand increases after 2020. This alternative will likely be the most common in the near future (although in the long run it is expensive) since most ships will not be able to have retrofits before or soon after 2020 [3].

If the EGCS alternative is opted, there are two different modes of EGCS, open-loop or closed-loop. Both cleans the flue gases, but the open-loop alternative dumps the polluted cleaning water into the ocean while the closed-loop collects the pollutants and discharges them for further treatment when in harbor. There are some drawbacks with EGCS though, since closed-loop is not possible for long voyages and the open-loop emissions to the ocean might be regulated in the near future. Also, it is costly to install the EGCS equipment on the ship [3].

The LNG alternative requires additional equipment for storing and distributing natural gas to the engines, and sometimes also new engines in case the old ones can not run on the combination of LNG and HFO [3]. Except for the high cost of installment, the lost space for cargo due to the LNG tank may also decrease profits. However, LNG is a cheap fuel, which in time will pay off for most types and uses of ships [1, 6].

The LNG alternative has been subject to intensive research the last decade and according to Xu et al. [7] there is an ongoing boom of the LNG industry globally. Still, further research can be made to improve the current LNG technology and in this work, the LNG fuel gas supply system (FGSS) is the subject to be studied.

1.1 Background

The adoption of natural gas as a marine fuel is becoming popular mainly due to the strict environmental regulations on the emissions coupled with its low price. Natural gas, which consists of mainly methane (CH_4) with minor amounts of other hydrocarbons (ethane, propane, butane and pentane) is stored in liquid form. The liquid form is achieved by lowering its temperatures to below its boiling point of approximately -162°C. This LNG is then stored and transported in special cryogenic tanks which are able to handle the low temperatures [8].

1.1.1 Original fuel gas supply system free of rotating equipment

One of the companies that offers marine FGSS of proven design is MAN Energy Solutions. Their existing system is free of rotating equipment which decreases the need of process maintenance. In this system, the LNG is transported from stationary bunker tanks into a cryogenic storage tank onboard the ship. To achieve sufficient insulation, the cryogenic storage consists of two containers with vacuum and perlite insulation in between. The inner container is in direct contact with the LNG and the outer container sometimes acts as a secondary barrier. Depending on the existing pressure and temperature inside the receiving tank at the time of bunkering, the LNG can be fed directly to the bottom of the tank to increase the pressure or sprayed from the top to decrease the pressure. The pressure increase from bottom filling is due to the compression of vapour by the increased liquid level while the top spraying pressure decrease is due to vapour being condensed by the subcooled LNG spray [9].

In this system, the LNG tank pressure is the main driving force for the delivery of fuel to the engines. To achieve this pressure, LNG in the tank is sent towards the pressure build-up unit (PBU) through the hydrostatic pressure difference between the top and bottom of the tank where it is evaporated with the help of a glycol-water heat exchanger [10]. After this, the slightly overheated vapor is returned to the LNG tank. The pressurized LNG is then pushed through a vaporizing unit (VAP) which vaporizes and superheats the LNG to an operating temperature that ranges between 10-30° C, the gas produced is then fed to the engines [9, 11]. It should be noted that before the gas is supplied to the engine, it passes through a Gas Valve Unit (GVU) whose main function is to regulate the feeding pressure to the engine and to ensure a fast and reliable shutdown of the gas supply [12]. A simple representation of the overall pump-less fuel system is shown in Figure1.1 below.

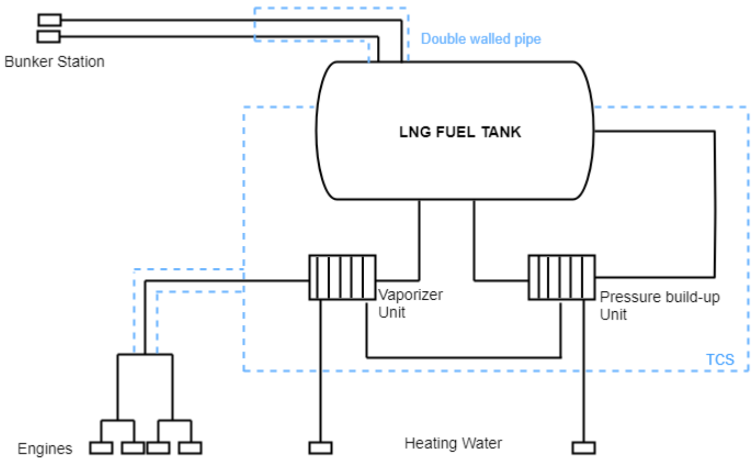

Figure 1.1: Illustration of the original robust design without rotating equipment [9].

The PBU works well in ships with small fuel tanks, but is limited by size when the LNG fuel systems are scaled up to fit the fuel consumption of larger vessels. This, together with changes in consumer requirements has led MAN Energy Solutions to develop two new fuel systems which will include rotating equipment, i.e. pumps and compressors. These two systems are described in Sections 1.1.2 and 1.1.3 below.

1.1.2 System 1

The first new system which will be referred to as System 1, is very similar to the previous one described in Section 1.1.1. The main difference is that this system will utilize a frequency-controlled standalone pump to supply the VAP. Apart from this, a recirculating line will be included to cater to minimum flow through the pump during start-up. An illustration of the system is shown in Figure 1.2. The illustration only shows one master valve and GVU, however the system is modeled with four engines and each engine will have its own master valve and GVU. The master valve is the last equipment within the FGSS, while the GVU is inside the engine system.

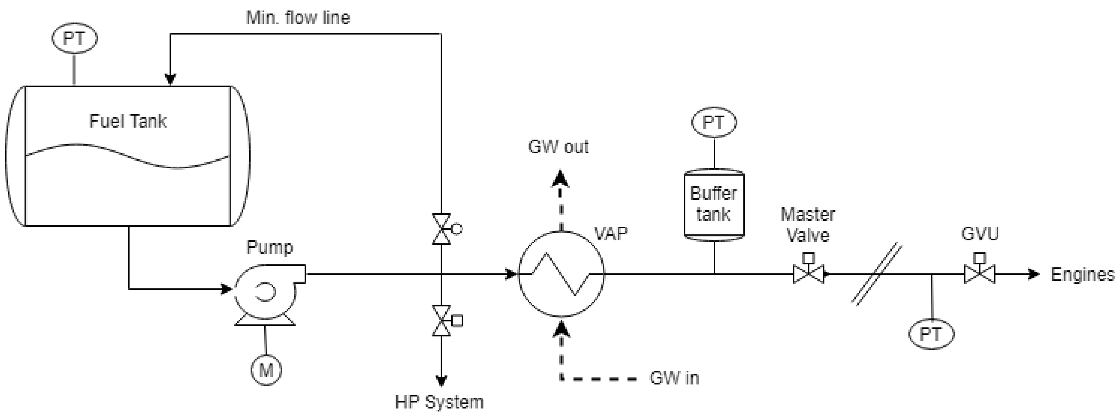

Figure 1.2: Illustration of System 1. The pump is submerged in a well, which is not shown in the figure. PT is short for pressure transmitter and the double dash after the master valve represents the end of the FGSS. The dashed lines are the glycol-water heating medium.

1.1.3 System 2

In the second system which will be referred to as System 2, a membrane tank will replace the conventional vacuum insulated tank. The membrane tank will be connected to a boil off gas (BOG) compressor and a submerged frequency-controlled centrifugal pump that will deliver the LNG to the engines (illustrated by Figure 1.3). Membrane tanks have less insulation than vacuum insulation tanks, which leads to significant production of BOG [10]. By IMO regulation, the gas in a tank can only be vented in case of an emergency (Email P. Dahl, 10 May 2019), this helps reduce greenhouse gas emissions. This together with fuel economy benefits is one of the main reasons that BOG utilization is implemented in this system.

The pump and BOG compressor produces a pressure which ranges from 3 to 8 bars depending on whether the engine is a dual fuel type or a pure gas engine [11]. However, it should be noted that the amount of gas obtained as BOG is low in comparison to the normal engine gas consumption [10] and therefore BOG is mainly used as a complementary fuel supply to the normal supply from the VAP and to feed the boilers in situations where the ship is idle. In this particular system, the VAP is fed by a submerged centrifugal pump which can be seen in Figure 1.3.

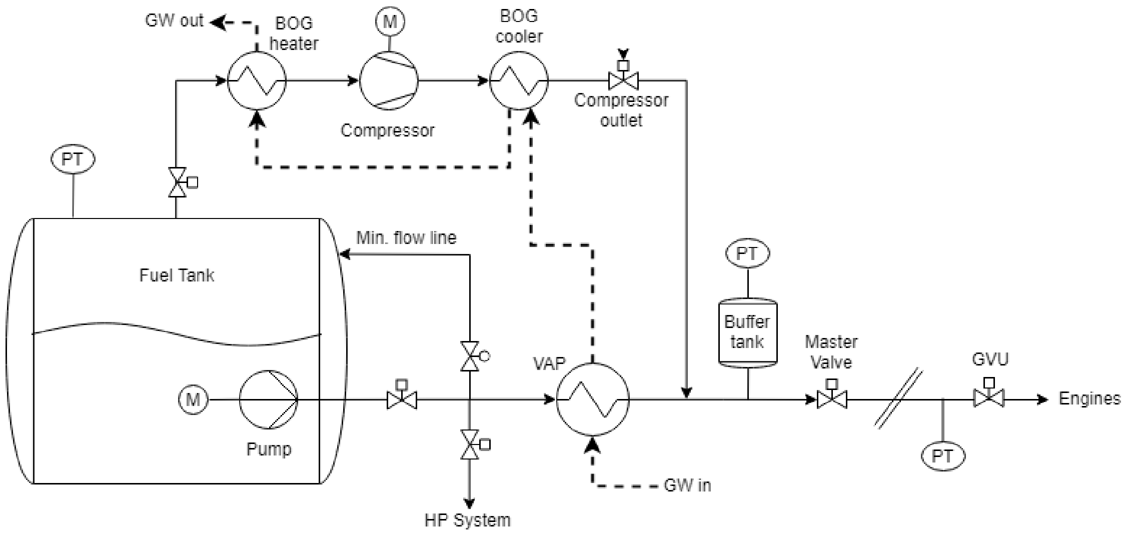

Figure 1.3: Illustration of System 2 which utilizes a submerged pump and a BOG compressor for fuel delivery. The dashed lines are the glycol-water heating medium and the double dash after the master valve represents the end of the FGSS.

1.2 Objective

The objective of this study is to examine the dynamics of System 1 which utilizes a vacuum insulated tank with standalone frequency-controlled pump (from Section 1.1.2) and System 2 which utilizes a membrane tank with a submerged frequency-controlled pump and a BOG compressor (from Section 1.1.3). More specifically, the dynamics being examined will be split into the following points:

1. Analyze the need of a buffer tank for a robust system.
2. Create a robust control strategy for the pumps and the compressor, which can handle fast changes in control signal or disturbances well.
3. Create a control strategy that handles the minimum flow over the pump at low engine load.

The objectives above will be evaluated for the scenarios A-E below:

A. Engine emergency load up from idle to full load
B. Engine emergency stop from full load
C. Engine fuel mode changeover from fuel oil to natural gas
D. Low tank pressure
E. Compressor startup

Scenarios A-C and will be investigated for both Systems. Scenario E will be investigated for System 2 because it is the only system with a compressor. On the other hand, scenario D will be concentrated on System 1 because the pump in System 1 is not submerged thus having the effect of low tank pressure more pronounced.

2. Theory

2.1 Centrifugal pump

Pumps are divided into two categories: centrifugal (kinetic) and positive displacement pumps. The selection of the right pump to use in a given process depends on different parameters such as: the liquid density, its viscosity, the presence of solids, liquid corrosivity, pressure differential across the pump and the liquid flow rate. Much concentration will be focused on the centrifugal pump because of its popularity in the process industries. A centrifugal pump is a device designed to move fluid from one point to another, this is achieved by transferring rotational energy from one or more driven rotors called impellers. During the transfer process, the fluid enters the rotating impeller along its axis and is cast out by centrifugal force along its circumference through the impeller's vane tips [13].

A centrifugal pump is an extremely simple machine that consists of two basic parts; the rotary element (impeller) and a stationary element or casing (volute). Its performance is described by a set of curves which are an important part of the design specifications. Pump curves are essential for the operation of the process because they indicate how a pump will perform in regards to pressure head and flow. Operating too far from the curve causes problems such as cavitation; which may lead to severe damages to the pump, an increase in energy consumption, and poor performance. Pump curves are plotted by drawing lines on points obtained from the pumps efficiency, shaft power, head and net positive suction head required ($NPSH_R$). $NPSH_R$ is the pressure measured at the centerline of the suction side of the pump and is needed for the pump to function satisfactorily at a given flow [14, 15].

2.2 Rotary vane compressor

The rotary vane compressor is a positive displacement compressor, meaning it compresses gas by enclosing a certain gas volume and then mechanically reduces the volume. Other typical positive displacement compressors are reciprocating piston or rotary screw compressors [16]. The rotary vane compressor consists of a cylindrical stator and a cylindrical rotor which has been offset in the stator, as can be seen in Figure 2.1. The rotor has slits containing sliding vanes which are pulled out against the stator wall by the centripetal force when the rotor is spinning. During operation, gas is drawn into the compressor just before the space between rotor and stator is at maximum and is then encased between two vanes. As the rotor is spinning on, the encased volume becomes smaller (due to the rotor offset) until the discharge port allows the compressed gas to exit the compressor [17].

The rotary vane compressor can be either oil-free or oil-injected, the oil-injected variant being more efficient and requiring less maintenance. However, a small amount of oil will slip by the compressor's oil separator which prohibits use of the oil-injected compressor in high purity gas systems [16]. Rotary vane compressors typically have a low-mid flow range of 100-20000 actual m^3/h and a low pressure ratio of up to 10 [18]. They have a simple design which gives them low capital and maintenance costs [19]. Due to low operation speed, rotary vane compressors only produce low levels of vibration which makes them have

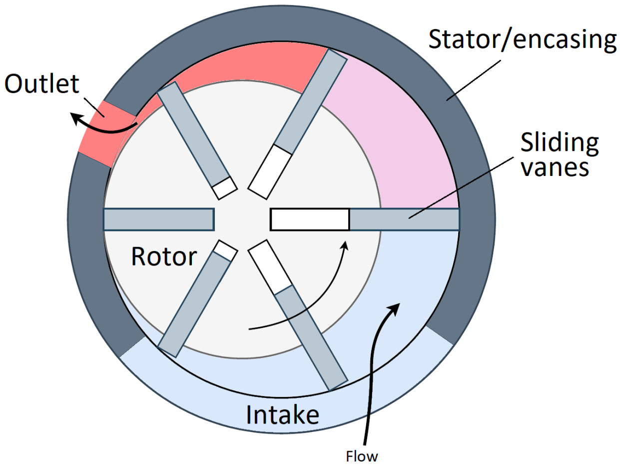

Figure 2.1: Schematic picture of the gas flow in a rotary vane compressor with six vanes.

low noise, low wear and in little need of maintenance. The rotary vane has a consistent performance through its service life since the vanes just goes further out as the stator wears out. However, two drawbacks with rotary vane compressors are that they have poor performance at high pressures and often are single-stage which gives them lower efficiencies than multistage compressors [20].

2.3 LNG storage tank

LNG storage tanks are specialized types of tanks that are manufactured with the ability to store cryogenic liquids [21]. In this project, two types of tanks are used, these include a vacuum insulated tank and a membrane tank. A vacuum insulated tank is in principle made up of two pressure vessels having one vessel installed inside another, with a vacuum maintained in the annular space between the vessels to help reduce heat transfer through convection [22]. This differs from the membrane tank which has a larger capacity and is non-self-supporting. It is surrounded by double hull ship structure and has less void space because it utilizes the hull shape. The membrane tank consists of a thin layer of metal which acts as a primary barrier, insulation and a secondary barrier and further insulation, these insure that the membrane is not stressed through thermal expansion or contraction hence increasing the protection of the hull structure from cryogenic spills [23].

One key issue with the membrane tank is its poor insulation, which results in high liquid boil off rate and consequently, pressure buildup. To avoid pressure buildup, it has been suggested to use the BOG to power auxiliary engines and boilers; but it should be noted that most of the times the power demand from these units far exceed the BOG from the tank. Thus, the BOG will mostly be a complementary source to the main fuel supply together with LNG which goes through the vaporizer (Personal communication MAN Energy Solutions, 11 Feb 2019).

2.4 Heat exchangers

Heat exchangers are used to transfer heat between hot and cold streams and are usually classified depending on the transfer process occurring inside them. There are many types of heat exchangers used in the process industry and their selection depends on many factors which include; capital and operating costs, fouling, corrosion tendency, pressure drop, temperature ranges, and safety issues (tolerance to leakage). In process systems, the main objective is to select a heat exchanger that provides the required heat duty (amount of energy to be transferred) for the hot and cold stream using the equations below;

$$Q = m\Delta H_{hot} \cong mC_P(T_{in}^{hot} - T_{out}^{hot}) \tag{2.1}$$

$$-Q = m\Delta H_{cold} \cong mC_P(T_{in}^{cold} - T_{out}^{cold}) \tag{2.2}$$

In addition to obtaining the heat duty, the overall heat transfer equation must be solved using;

$$Q = UA\Delta T_{LM} \tag{2.3}$$

Where U is the overall heat transfer coefficient which represents the ease with which heat is transferred between the mediums. U is a function of not only the material and shape of the heat exchanger but also the fouling and the flow regime. A is the heat transfer area, which is calculated based on specifications of the dimensions of the process streams contact area and (ΔT_{LM}) is the log-mean temperature difference. The equation is only valid when simple counter or co-current flows exist in the system. In addition, it should be noted that there exists a pressure drop in the heat exchanger due to friction as the fluid flows through the unit, correlations such as Beggs-Brill can be used to calculate such pressure drops [24].

Several heat exchangers exist and are classified according to their flow path, configuration and the phases of the fluid. Amongst the existing heat exchangers, the most commonly used is the shell and tube type. For this heat exchanger one fluid flows in the tubes whilst the other flows in the surrounding shell. Some of the advantages that come with using this type of heat exchanger are its abilities to operate at high pressures and its flexibility towards phase changes[25].

2.5 Valves

Valves are devices used to direct, start, stop, mix and regulate fluid flows [26]. They can be classified depending on function, application, motion and port size, but the function description suffices here. It divides valves into on/off, non return and throttling valves. On/off valves are only used to either block or let flow through and they are typically hand-operated but can also be automated. On/off valves are probably the most common valve type in a process since they are often put around other equipment which may need maintenance and since relief valves and safety valves also are included in the on/off category. Non return valves are used to restrict flow in one direction only, often to protect rotating equipment such as pumps and compressors. Throttling valves are used to adjust flows, temperatures and pressures of streams. These are nowadays typically automated with actuators coupled to control systems, but can also be hand-operated.

Valves are sized by the valve coefficient (C_v) which affects the volumetric flow (Q) through the valve according to the simplified Equation 2.4 below;

$$Q = \frac{C_v}{m} \cdot \sqrt{\frac{\Delta P}{SG}} \tag{2.4}$$

where m is a valve dependent coefficient, ΔP the pressure drop and SG the specific gravity of the fluid [26]. A valve is also distinguished by the flow characteristic, which is how the flow and pressure through the valve behaves depending on the stroke opening degree. There are three general flow characteristics: quick-opening, linear and equal percentage, where equal percentage is most common. The inherent flow characteristics of the equal percentage stroke are non-linear, but they often become somewhat linear when taking piping effects into account. Valves with linear stroke are similarly pushed towards the non-linear quick opening characteristic by the piping effects. Linear flow characteristics are preferred to achieve good control of a process since most controls are linear [27].

2.6 Piping

Process piping is one of the most important components of a process. Pipes are generally used to transport fluids (liquids and gases) safely and efficiently from one piece of equipment to another. The material used and sizes of the pipes vary according to their required area of use and the type of fluid being handled. The greatest effect that pipes have on a process are their ability to reduce the fluid pressure which occurs because of frictional resistance to flow from the pipe wall, fittings and bends but also from within the fluid itself. There can also be pressure gain or loss between the start and the end of the pipe which may be caused by pipe elevation [28], which is called hydrostatic loss. There is also a kinetic pressure loss in pipes, but it is most often negligible compared to the other losses [29]. These three types of pressure losses are presented in Equation 2.5 below;

$$\Delta P_T = \Delta P_{HH} + \Delta P_f + \Delta P_k \cong \Delta P_{HH} + \Delta P_f \tag{2.5}$$

where ΔP_T is the total pipe pressure drop, ΔP_{HH} the hydrostatic pressure drop, ΔP_f the frictional pressure drop and ΔP_k the kinetic pressure drop. There are many proposed correlations in literature to model pipe flow (ΔP_{HH} and ΔP_f) such as Beggs & Brill, Gray and Petalas & Aziz [30, 29]. Some of them are based on locating the operation flow regime to account for flow and holdup in all directions while other correlations only work in more specific conditions.

The propagation of a pressure wave in a pipe goes with the speed of sound in the specific medium [31]. Thus, the time it takes for a system to detect a change in fluid pressure in a pipe, due to closing valves or altered equipment speeds, will be the quotient of distance to origin and the speed of sound. In natural gas, the speed of sound is roughly 400 m/s [32, 33] and pressure changes in a system shorter than a couple hundred meters will therefore happen in less than one second.

2.7 Buffer vessel

Buffer vessels are intermediate storage tanks which are used between and within processes to provide smooth operation [34]. More specifically, they are used to mitigate disturbances and/or to provide independent operation between unit operations. Disturbances such as variations in flow, pressure or temperature, are dampened by the holdup volume of the buffer, analogously to integrators in control theory. The allowance of independent operation includes for instance; changeover between batch and continuous processes, temporary shutdowns [34] and momentary overloads [35].

2.8 Mixers and tees

Mixing is a complex process which is hard to rigorously model [36] but in HYSYS it is assumed the flow is fully mixed and the calculation is made only using regular mass and heat balances. The mixer pressure can be set to the lowest of the mixer inlets but in dynamic mode HYSYS recommends to use an option which equalizes all pressures, giving all streams connected to the mixer the same pressure. The dynamic mixer is modeled without any holdup volume and variations in the inlet will therefor appear instantaneously in the outlet [30].

Tees are used to split streams and in HYSYS they are essentially modeled the same as mixers but backwards. The same balances and pressure specifications are made and when experiencing backflow in dynamic mode, a mixer behaves like the tee [30].

2.9 Control theory

Most chemical, mechanical and physical processes are dynamic by nature and do therefore need to be controlled to produce the desired result [37]. This is done with process control, which may be more or less advanced. A very simple example is the thermostat control of a heat element, which turns the heat on when it's too cold and turns it off when it has achieved the set temperature. However, on-and-off control like this is not enough to keep most processes at stable satisfactory levels and more elaborate control methods are used.

2.9.1 Feedback control

A very important controller type in industry due to its simplicity and effectiveness is the proportional-integral-derivative (PID) controller [38]. It uses a feedback loop to calculate the error between the set point and measured output. In proportional control, the error is multiplied with a constant to decide the controllers' action on the process; a high proportional constant makes the change quicker but also less stable. In integral control, the error is integrated backwards in time which deletes the lasting error that proportional control experiences. This however comes to the cost of oscillatory behaviour and lowered stability. Integral control can also suffer from windup in saturated systems and needs anti-windup measures to function safely. The last control, derivative control, calculates the error time derivative to anticipate future changes and give faster response. In cases without heavy measurement noise, derivative control increases the stability of a PID controller. Equation 2.6 below show the ideal control equation of a PID controller [38];

$$u(t) = K_c\left(e(t) + \frac{1}{\tau_I}\int_0^t e(x)dx + \tau_D\frac{de(t)}{dt}\right) + u_{ab} \tag{2.6}$$

where $u(t)$ is the control signal, t the time, K_c the proportional gain, $e(t)$ the error, τ_D the derivative time constant, τ_I the integral time constant and u_{ab} the actuator bias signal.

The PID controller is a linear type of control, which assumes that the process is close to linear around the operation point to work properly. Also, it was mentioned before that integral control needs anti-windup measures to work properly in saturated conditions [38]. One such measure is to rewrite the PID equation into velocity form [39, 40], see Equation 2.7, which calculates the control signal rate of change before the integrator. When saturation occurs, this rate of change will be zero which cancels the integrator and yields the anti-windup effect sought for.

$$\frac{du(t)}{dt} = K_c\left(\frac{de(t)}{dt} + \frac{1}{\tau_I}e(t) + \tau_D\frac{d^2e(t)}{dt^2}\right) \tag{2.7}$$

2.9.2 Feedforward control

Feedback control is good at restoring system operation from disturbances but it cannot adjust for disturbances in advance. To do this a control method called feedforward control can be used. Feedforward control is based on measuring the disturbance before it hits the process and adjust the process parameters just in time of the disturbance to mitigate the disruption to the process [38]. A control scheme of a feedforward loop added to a feedback system is presented in Figure 2.2 below.

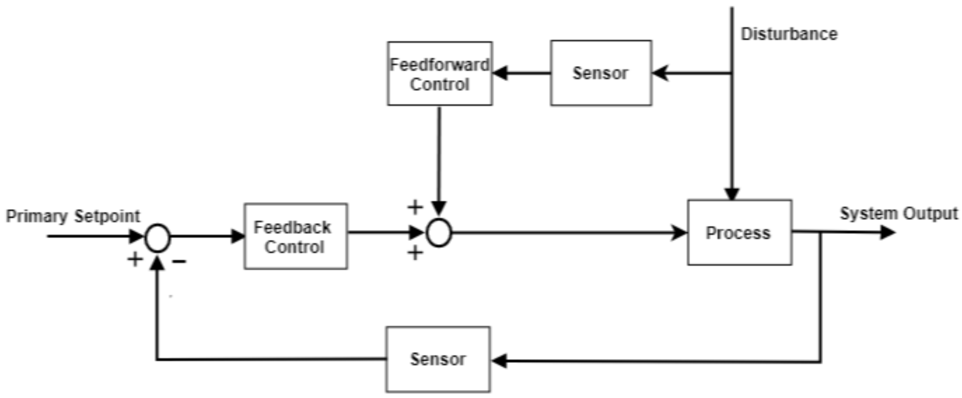

Figure 2.2: Combined feedback and feedforward control scheme.

The feedforward transfer function $G(s)$ is often on the form of Equation 2.8 below [30],

$$G(s) = K_p\frac{(\tau_{p1}s + 1)^{-ds}}{\tau_{p2}s + 1} \tag{2.8}$$

where the parameters are feedforward gain K_p, delay time d, lead time constant τ_{p1} and lag time constant τ_{p2}. The transfer function is then multiplied with the feedforward signal and added to the ordinary control signal [30]. The delay time is used if the control action is much quicker than the disturbance whilst the lead and lag time constants are used to time the control according to the lag between control output and process variable respectively disturbance and process variable [41].

2.9.3 Cascade control

Cascade control is another way to mitigate the effect of disturbances to a process. It does this through two feedback loops, one inner and one outer, measuring two variables instead of just one. The outer loop is similar to the traditional feedback loop, comparing the process output to a set point, but instead of changing a process variable it produces the set point of the inner loop (see Figure 2.3). The inner loop then compares this set point with a secondary process variable and produces the control output which affects the process variable [38]. If the inner loop is much faster than the outer loop, it can respond to the disturbing process variations more quickly than just the original outer loop would have done on it's own. The fast inner loop also linearizes the control variable behaviour, resulting in more accurate control of the main variable that the outer loop is measuring. However, if the inner loop is too slow compared to the outer loop, cascade control can instead result in instabilities [42].

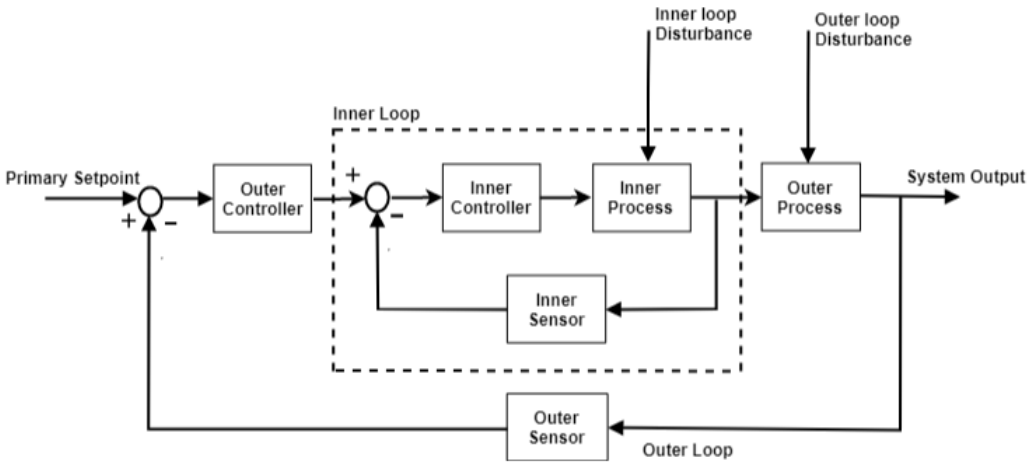

Figure 2.3: Cascade control scheme.

3. Modeling

This chapter describes some model specific theory and how the modeling was performed. First, a steady state simulation with all the basic functions of the system was built. This was then converted into a dynamic simulation with the help of the HYSYS Dynamics Assistant, changing the boundary conditions to pressure specification in all inlet and outlet streams as well as some equipment unique steady state/dynamic settings. All major settings used will be mentioned while minor settings will only be brought up in the case of deviation from the Aspen HYSYS V10 defaults. All graphs have been made in Matlab R2017b.

3.1 Equation of state

One important aspect of computational modeling of gases and liquids is the utilization of proper equations of state which yield accurate results of the certain compounds and conditions modeled. In this project, temperatures ranging from -182°C to 175°C and pressures between 1 and 10 bar were employed. The substances included are LNG (composition in Table 3.1), water and ethylene glycol. Only LNG is present in both liquid and gaseous phase while the others are always in liquid state. The LNG is stored in cryogenic conditions and is relatively close to the triple point (-182.5°C, 0.117 bar) but way below the critical point of (-82.6°C, 46.0 bar)[1]. The gases however are high above the critical temperature but way below the critical pressure.

According to literature [43, 30], the Peng-Robinson (PR) model is favorable for vapour-liquid equilibrium calculations for hydrocarbon systems below critical conditions. According to the Aspen HYSYS V10 help manual the Peng-Robinson model is reliable down to temperatures of -271°C and pressures up to 1000 bar. Other models for hydrocarbon systems such as SRK, PRSV and Chao Seader were also considered but turned down in favour of the PR model. However, for non-ideal systems such as the glycol-water system in this project, PR is not the most accurate and activity models such as Wilson, NRTL and UNIQUAC were reviewed. These three models produced similar results in the glycol-water system and NRTL was chosen since it is computationally lighter than UNIQUAC and tantamount to Wilson [30, 44], thus making the dynamic simulations go faster.

Table 3.1: The LNG composition in vol% and mol% (at -162°C and 1 atm) [45] and the resulting BOG composition in mol% at -155°C and 1.1 bar which were used in the project.

Compound	LNG vol%	LNG mol%	BOG mol%
Methane (C_1)	94.0	95.88	95.53
Ethane (C_2)	4.7	3.04	0.01
Propane (C_3)	0.8	0.50	0
n-Butane (C_{4+})	0.2	0.11	0
Nitrogen	0.3	0.47	4.46

[1] The triple and critical points of methane, which makes up 96 mol% of the LNG.

3.2 Holdup volume

In dynamic simulations, equipment with volume such as heat exchangers, pipes and separators have to model the accumulated fluid(s) inside their holdup volumes. Basically, the accumulated material is calculated by adding the inlet flow with a theoretical recycle of the holdup minus the outlet flow. The inlet material is flashed and mixed with the holdup to a degree (or efficiency), which may be specified in HYSYS. In this project, these efficiencies have been kept at the default value of 100%. The holdup of pipes is different and there is no possibility of changing mixing efficiencies within them. The calculations being made are about the accumulation of material and energy, thermodynamic equilibrium, heat transfer and chemical reactions [30].

3.3 Pump

The most important part in the FGSS is the pump. In HYSYS' pump calculation block there is no possibility to select what type of pump to simulate. Instead, any unique pressure-flow behaviour is decided by the characteristic curves that may be used in the pump. In this work, the P-H and NPSH_R curves of a representative pump were available from a product specification and entered into HYSYS. These curves can be found in Appendix A. The inertia of the pump, I_p, (kgm^2) was estimated using HYSYS formula of Equation 3.1 [30],

$$I_p = 0.03768 \cdot \left(\frac{P}{\omega^3}\right)^{0.9556} \tag{3.1}$$

where P is power in kW and ω is rotational speed in rpm/1000. The electrical motor inertia has a similar formula (Equation 3.2) using the same units.

$$I_m = 0.0043 \cdot \left(\frac{P}{\omega}\right)^{1.48} \tag{3.2}$$

The inertia estimations resulted in 0.00266 kgm^2 for the pump and 0.05385 kgm^2 for the electrical motor. The figures used to calculate the inertia can be found in Appendix A, together with all other relevant figures for the pump. The dynamic specifications of the pump were "Use characteristic curves" and "Electric motor", which are recommended by HYSYS to use when including an electrical motor. The electrical motor model used is called "breakdown" model, which makes use of the speed-torque curve both during startup, shutdown and normal operation. It can reduce the speed if the system torque or resistance becomes too large and grants smooth transitions when in operation [30]. The speed-torque curve is default, except for the last point (96.66%, 170%) which was required for the breakdown model to function. Also a setting called "typical operating capacity" was used, which can help startup modeling by increasing the density of the fluid if the flow becomes less than 0.2% of the typical operation capacity. Lastly, a gear factor between the pump motor and pump was used. It was calculated by dividing the pump maximum speed with the maximum speed of the motor.

3.4 Compressor

The compressor to be modeled is an oil-injected rotary vane compressor, which uses lubrication oil to cool down the compressor. However, since HYSYS have no computational block for rotary vane compressors, the compressor was simulated as a screw compressor.

This is also a rotary compressor of the positive displacement type, but it has some differences towards rotary vanes. Since no accurate performance curves were available for the compressor the rest of the settings were kept at default as the detail of the compressor dynamics would not be very close to the real rotary vane compressor anyway. The dynamic specifications of the compressor were set to adiabatic efficiency and speed.

3.5 Heat exchanger

Several heat exchanger models can be used in HYSYS, some of these include; End point analysis model, Steady state rating method and a Dynamic rating method which operates well in dynamic simulation. For this process, the basic dynamic rated shell and tube heat exchanger model was used because of its ability to function well in dynamic simulations. For the initial set up of the VAP, the volumes and pressure drops were specified according to a 1200kg LNG/h heat exchanger. For the BOG heater and cooler these parameter values were halved, see Table 3.2 for all heat exchanger input. These specifications made it possible for the overall conductance UA, k-value and the total heat transferred between the shell and the tube side to be calculated by the program.

In Aspen HYSYS, the basic heat transfer model is the same for the shell and tube side except for the shell having the additional term of heat loss to the surroundings. As no heat loss model was included in this work's heat exchangers, the selection of which fluid to have in the tube side or shell side had no significance. However, the heating medium mixture of 50-50 mol% water-ethylene glycol was chosen to the shell sides of all heat exchangers while the hydrocarbons were put in the tube sides. The heating medium had the temperature of 50°C at the VAP inlet and exited the last heat exchanger, the BOG cooler, at around 40°C.

Table 3.2: The volumes and pressure drops of the heat exchangers.

Heat exchanger	Shell ΔP (kPa)	Tube ΔP (kPa)	Shell volume (liter)	Tube volume (liter)
VAP	80	10	30	20
BOG heater	40	5	15	10
BOG cooler	40	5	15	10

3.6 Valves

Control valves with linear actuator speeds obtained from 2.4 were used. Linear control valves have flows which are directly proportional to the percent opening i.e $\%C_v = \%Valve\ Opening$. To perform their required tasks efficiently, the valves were sized according to HYSYS universal method using equation 3.3 for the gaseous phase and equation 3.4 for the liquid phase.

$$f(lb/hr) = \upsilon_{fracfac} 1.06 C_g \sqrt{\rho(lb/ft^3) \times P_1} \times sin(Argument) \tag{3.3}$$

$$f(lb/hr) = (1 - \upsilon_{fracfac}) \times 63.338 \times C_v \times \sqrt{\rho(lb/ft^3)} \times \sqrt{P_1 - P_2} \tag{3.4}$$

Where the Argument is a constant derived from C_v and C_g, P_1 is the pressure of the inlet stream, P_2 is the pressure of the exit stream without static head contributions and

$v_{fracfac}$ is the outlet molar vapor fraction. Variables such as; stream inlet and outlet pressure, temperatures and valve pressure drop can be specified but for full operation only three of the mentioned variables are required[30]. For this process, the specified variables varied according to the operation stages. Also, the valves can have actuator speeds specified, these are show in Table 3.3.

Table 3.3: Valve actuator percentage speed depending on pipe size and stroke length, based on an assumption of 3-4 mm/s actuator speed.

Pipe size (DN)	10	15	25	32	40	50	65	80	100
Stroke length (mm)	10	10	9	9	11	15	23	23	30
Min. linear speed (%/s)	30	30	33.3	33.3	27.3	20	13	13	10
Max. linear speed (%/s)	40	40	44.4	44.4	36.4	26.7	17.4	17.4	13.3

3.7 Control

In HYSYS, normal process control is put in using PID controllers, which has a lot of built in functions such as autotuning, alarming and feedforwarding. The controllers can be put in four modes; off, manual, auto and indicator and the action of the controller can be set to reverse or direct, depending on the process and placement of the controller [30].

3.8 Pipes

For the pipe modeling, Beggs and Brill (1979) correlation was used because of its ability to include both frictional pressure drop and liquid holdup corrections for uphill and downhill [30]. All the pipes included in the system were assumed to be made of stainless steel with a universal roughness of 0.045mm and conductivity of 16.50W/m-k (Personal communication from ÅF). Other properties of the pipes such as; the pipe length, insulation and the diameters were obtained from literature compiled by MAN Energy Solutions. A summary of the extracted pipe information for both systems is shown in Table 3.4.

Table 3.4: List of pipes and related properties

From	To	DN(mm)	Length (m)	Insulation type	System
Tank (LNG)	Pump	100	30	Double walled	1
Pump	VAP	50	20	Double walled	1, 2
Tank (GNG)	BOG-Heater	65	18	Single walled	2
BOG-Heater	Compressor	100	5	Single walled	2
Compressor	BOG-Cooler	100	2	Single walled	2
Master Valve	GVU	100	15	Single walled	1, 2

3.9 GVU and engines modeling

The suction created by an engine could be modeled and included in a dynamic simulation, however it was outside the scope of this study. Instead, only the GVU was modeled as a valve with the outlet pressure 4.7 barg (the suitable engine inlet pressure for 100% engine load) and a pressure drop of 0.6 bar. The exception to this pressure specification was during the loadup scenarios, where the engine gas lines were evacuated to atmospheric pressure. Accordingly, the outlet pressure was set to 1.013 barg during the loadup scenario.

4. Results and discussion

The following chapter presents the results of the dynamic simulations, intertwined with remarks and analysis of the results. The majority of the results come from simulating the scenarios and these results will be presented in separate sections.

4.1 Process control development

As one part of the thesis scope, a functioning control system was developed and tested for the low pressure FGSS. One criterion was to avoid the use of a flowmeter to lower the cost of the FGSS and instead rely on pressure sensors to provide the correct gas flow to the engines. The philosophy during the control development was to build the control system as simple as possible but still effective at meeting set points and mitigating disturbances. Essentially, there were two different missions for the control system in this work. The most important was to supply sufficient flow to the engines within a certain pressure range and the other was to try to keep the tank pressure in check (does only apply for System 2).

The LNG flow was regulated by speed control of the pump, via a feedback of the GVU inlet pressure. As long as the pump provided the right amount of flow at steady operation, the pressure stayed around the set point. When the engines sped up and consumed more gas, the GVU pressure went down, causing the pump to speed up and deliver more flow to meet the pressure set point. A PI controller was constructed for the feedback loop, but the tuning of the controls in System 1 and 2 were made separately and their different PI parameters can be found in Table 4.1. PI control was chosen since it is simpler than PID control and due to the fact that at the time of the control construction, the simulation had issues with rapid fluctuations which potentially would be problematic for the derivative control to handle. The pump control in System 2 was tuned with HYSYS autotuning function but the resulting tune was a bit too unstable and had its gain reduced to increase stability. The control of System 1 was only based on the pump control, resulting in the control design in Figure 4.1.

In the case of System 2, the tank pressure was controlled by the compressor, using speed control with a pressure feedback from the tank. Also, the compressor outlet valve was set to close in the case of satisfactory tank pressure when the compressor shuts down. However, since the LNG tank was not simulated in this study, the compressor speed was manually controlled to either produce a flow of around 400 kg/h or to be shut off.

Some System 2 simulations were also run with feedforward of the compressor speed to the pump control, to increase the response of the pump speed towards compressor flow changes. The feedforward signal was constructed to reflect the BOG flow to the GNG line, by multiplying the compressor speed with the opening degree of the compressor outlet valve. Thus, the feedforward signal was zero when the valve was closed, even though the compressor might have been running to build up pressure. In the simulations, the time parameters were kept at zero for simplicity and the gain was given a rough tuning to K_p=-0.035 based on a couple of feedforward tests. A more aggressive K_p of -0.07 was also used earlier, which gave faster response but overshot the feedforward control.

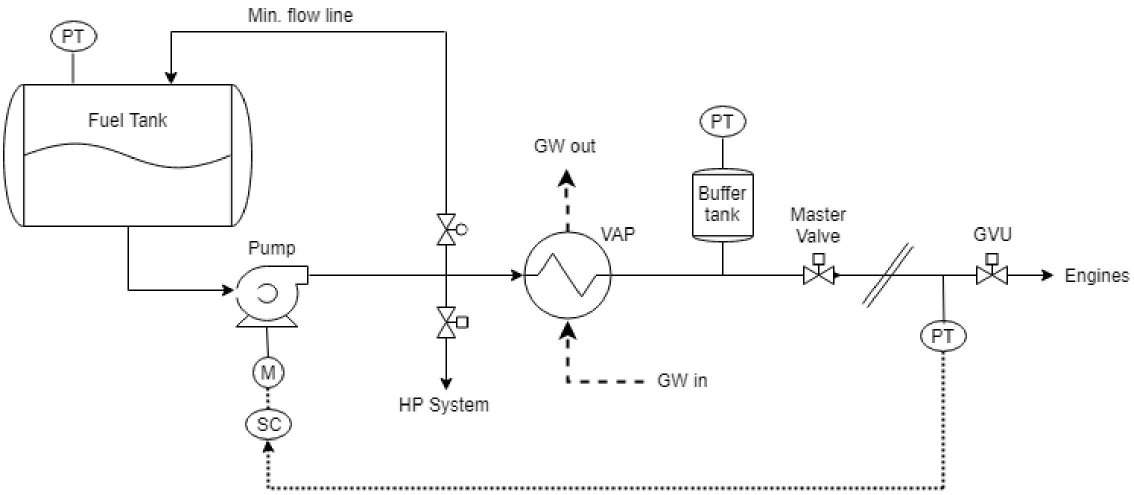

Figure 4.1: The control system design of System 1, with streams in filled lines and control signals in dashed lines.

In the simulation the GVU also had to be controlled even though in reality that control was within the engine supplier's process and outside of the FGSS. The GVU was simply simulated as a valve with flow control, using the PI parameters in Table 4.1.

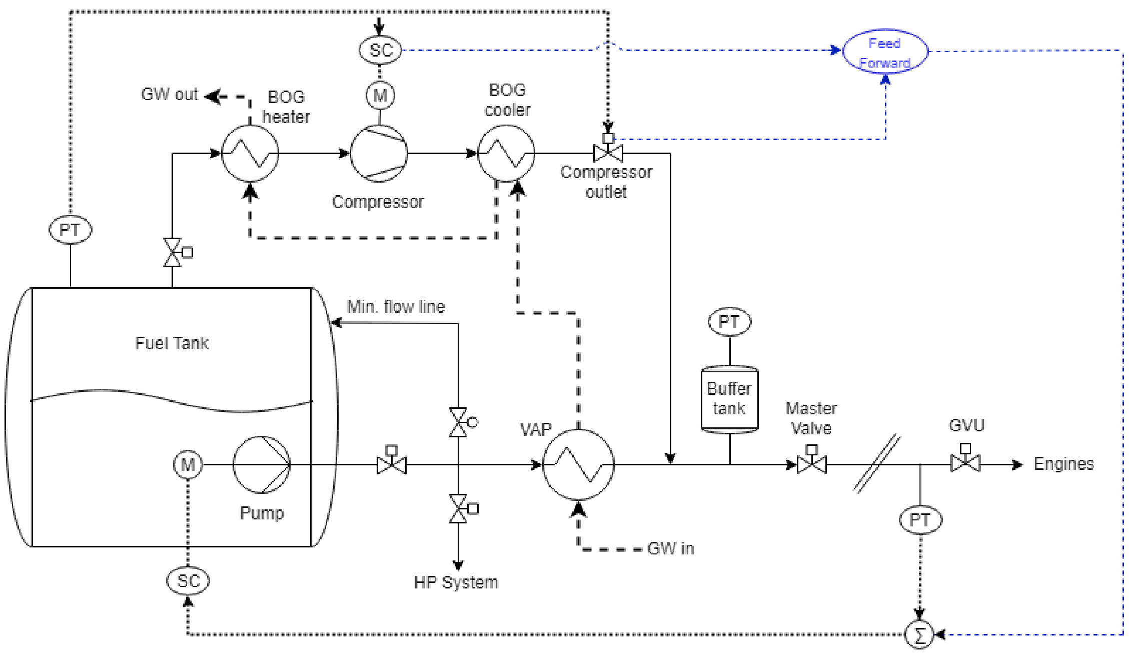

Figure 4.2: The control system design of System 2, with streams in filled lines and control signals in dashed lines.

Outside the scope of this study, but with importance for the real process is the control of the LNG feed to the HP pump system. In this simulation, the HP stream flow was controlled with a valve aiming for a flow of 6000 kg/h. The dynamics of the HP stream flow controller will not be examined but the HP stream is only included in the simulation to provide a correct size of flow in the pump. The flow controller PI parameters can be found in Table 4.1.

Table 4.1: PI-control parameters of the various controllers used in the simulations.

System 1	K_c	T_i	System 2	K_c	T_i
Pump	0.05	1.0	Pump	2.0	0.623
HP	0.05	1.0	HP	0.5	1.0
GVU	0.05	1.0	GVU	0.8	0.6
Comp	-	-	Comp	0.8	0.6

4.2 Emergency loadup and fuel changeover

Emergency loadup and fuel changeover are scenarios in which the FGSS is activated to go from idle mode to full speed. The difference between the two are mostly the startup rate; the emergency loadup is supposed to reach full load in 150 seconds and the fuel changeover is supposed to reach full load in 50 seconds according to the engine manual. Because the scenarios are similar, only the fuel changeover was simulated since it places higher demands on the FGSS. The simulation will henceforth be mentioned as "loadup" and it will also be the same for both systems, since the compressor was not included in the loadup of System 2.

Before the loadup, the FGSS was in idle mode, meaning the pump was running at minimum speed and all flow was recirculated to the tank. Also, the line between the master fuel gas valve and the engine had previously been evacuated and contained gas at atmospheric pressure. The loadup began by opening the master fuel gas valve and setting the pump control to AUTO. As the GVU pressure reached the set point pressure of 5.3 barg, the GVU was linearly opened to the full load opening degree in 50 seconds and the recirculation was closed over 35 seconds. The resulting flows can be seen in Figure 4.3, where time zero was the start of the loadup. At the end of the GVU ramp the GVU flow was 2540 kg/h and 2.3 minutes later it reached 2590 kg/h. This indicates that the pump control is not quite fast enough to erase the last few percent of error in a reasonable time.

The flow spike at time zero in Figure 4.3 was due to the GVU pressure being atmospheric before the master gas fuel valve opened up, making the pump control accelerate quickly. Also, there are a lot of control fluctuations in the VAP outlet at time when opening the GVU. These are presumably due to both pump control fluctuations and numeric fluctuations over equipment with too small pressure drop (most likely valves in the LNG/GNG-line).

The pressures of the pump, VAP, pump recirculation and GVU during the loadup can be seen to the left in Figure 4.4. A loadup scenario was also performed of the system equipped with a 2 m^3 buffer tank. It should be mentioned that The volume of the vessel was based on direct communication obtained from MAN Energy Solutions, who stated that the required vessel volume be between 2 to 3 m^3 and at most 5 m^3 . This volume range is the acceptable volume range for the TCS (Personal communication from Peter Dahl, 7 May 2019). The results from this loadup experienced pressures almost identical to the original system.

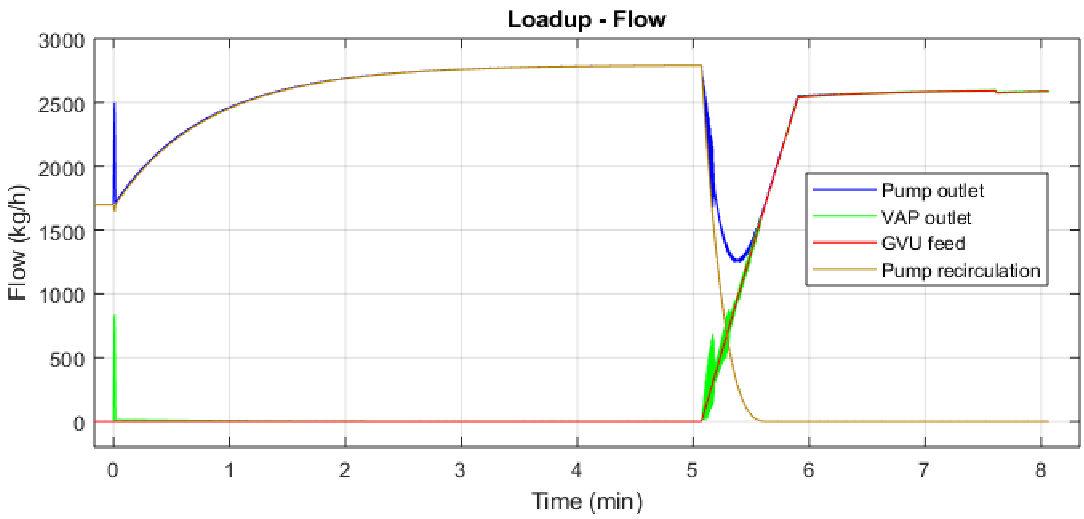

Figure 4.3: Mass flow during the loadup scenario.

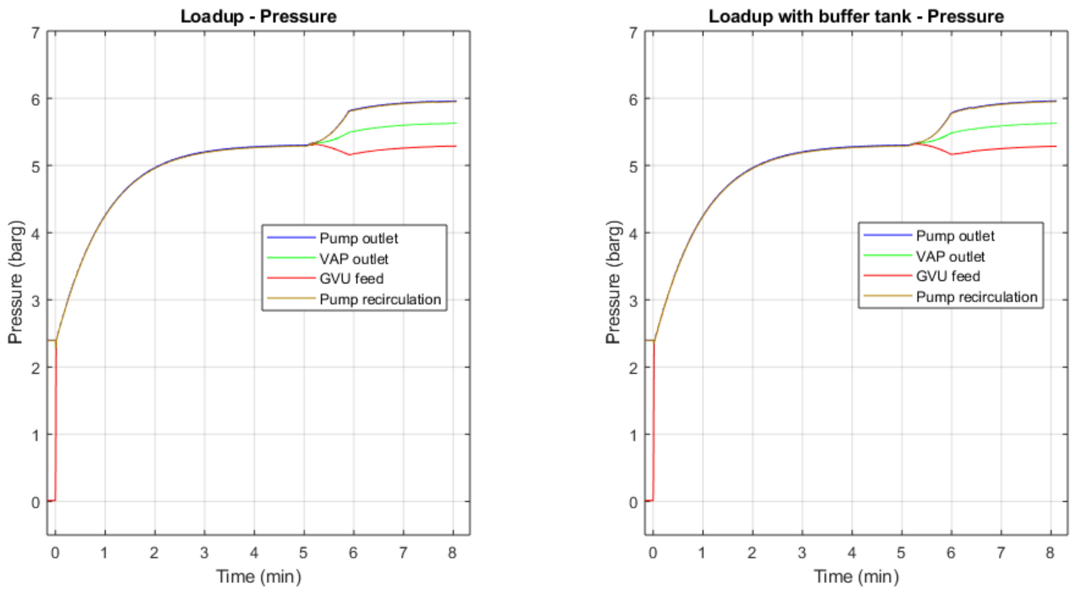

Figure 4.4: System pressures during the loadup, the original system to the left and the buffer equipped system to the right.

The flows of the buffer equipped simulation are presented in Figure 4.5, where the filling and discharge of the buffer vessel can be seen as the difference between the green and red lines during the first respective five minutes.

The overall pressures were similar in both simulations, but if the GVU pressure is zoomed in at the time of opening the GVU, then the delaying effect of the buffer is just barely visible. This is presented in Figure 4.6, where the typical buffer effect of slowing down pressure changes can be seen. Time zero in this figure refers to the time of opening the GVU and closing the recirculation. The GVU feed turning point in the bottom occurred as the GVU valve finished its ramp and the notches in the GVU feed curve at time 1.25 minutes respectively, the changes that occurred at 2.5 minutes were due to the GVU control being changed from manual to automatic. The automatic GVU control adapts the system faster, which makes the buffer delay effect non-visible after minute 1.25.

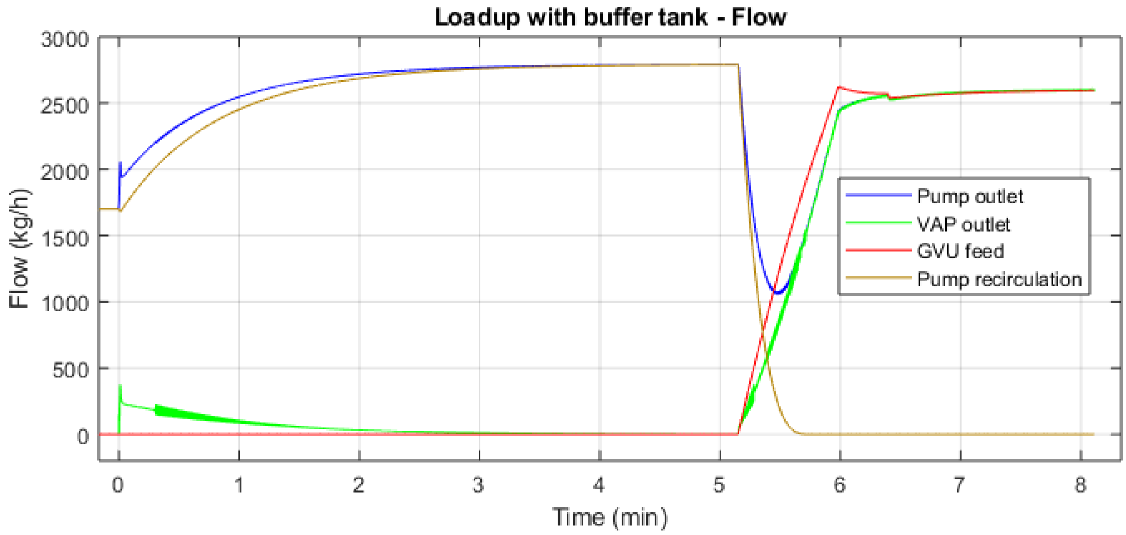

Figure 4.5: Mass flows of the system equipped with a buffer vessel during loadup.

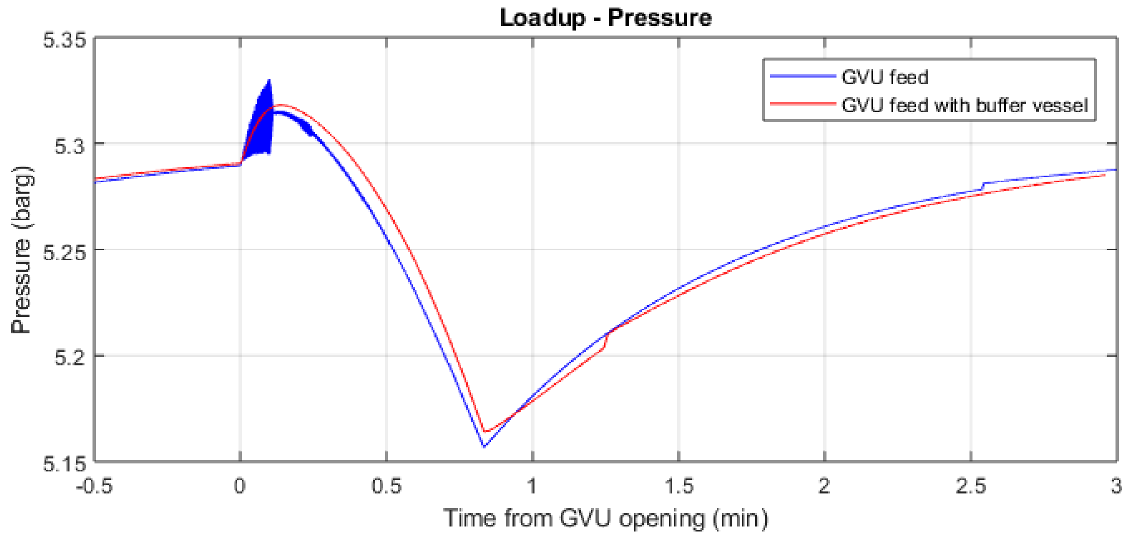

Figure 4.6: GVU feed pressures during the opening of the GVU, for both the original system and the buffer equipped system. At time zero the GVU is beginning to open and the recirculation beginning to close.

4.3 Emergency shutdown

An operational and effective shutdown process is essential to protect human life, prevent extensive equipment damages and adhere to regulations. The emergency shutdown system (ESD) is a process designed to minimize the consequences that may arise from various emergency situations such as equipment failure, tank high pressures, cryogenic leakages and fire outbreaks; which, if not controlled, can be hazardous. Typically, what is expected in an ESD is the immediate shutdown of major equipment and supporting systems in minimum time. For this process, it is required that the flow of both the LNG and the GNG are stopped without exceeding the designed limits.

4.3.1 Emergency shutdown - System 1

Prior to the emergency shutdown, the pump was in operation and fuel was delivered to both the engine and the HP feed. When the emergency shutdown was initiated, all open ESD valves were closed. In the simulation of System 1, this means the pump inlet and the master fuel gas valves were closed. Additionally, the HP feed valve and GVU were closed while the pump was shut off by shutting off the power with an on/off controller and deactivating the PID controller. The resulting flows and pressures of the emergency shutdown can be found in Figure 4.7.

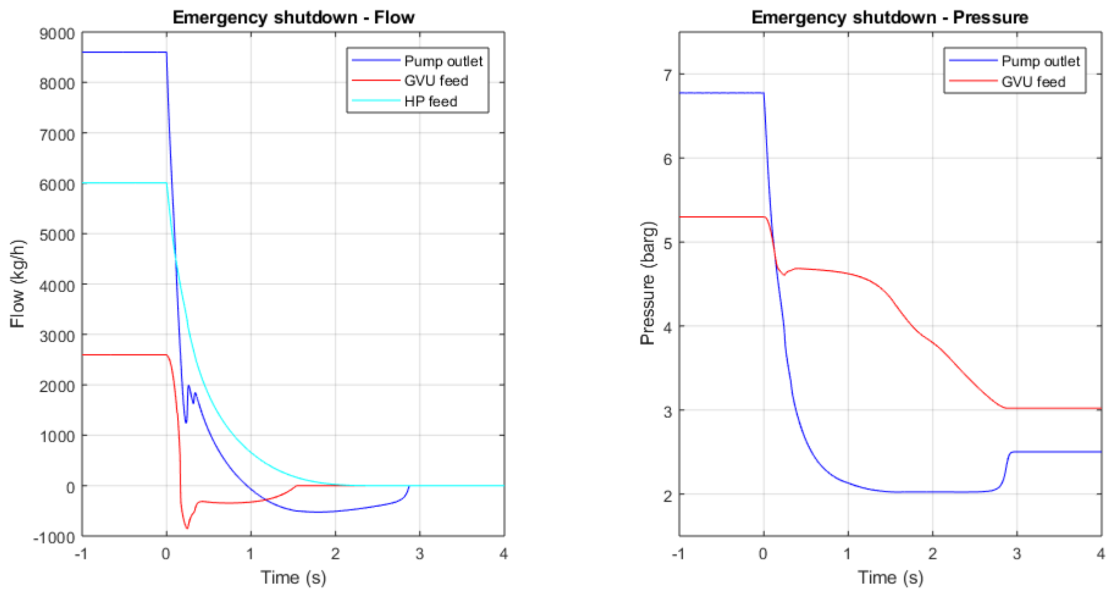

Figure 4.7: The flows and pressures in System 1 during the emergency shutdown, which started at time zero. Mass flows (kg/h) to the left and pressures (barg) to the right.

From Figure 4.7 it can be noted that the GVU flow was reversed in just 0.2 seconds and the pump flow was reversed after 1 second. Also, the HP feed stream had a slower decline than the others, which is due to the pressure specification after the HP feed valve being the lowest of the outlets in the system at just 0.5 barg. The HP feed valve inlet pressure however is of the same pressure as the pump outlet and is therefore not shown in the pressure diagram. No pressure spikes were observed, likely due to the valve closing times of a couple of seconds allowing the pressure escape back into the tank and the high pressure system (HP feed). The high pressure system would in reality not have the possibility to do this and should have had higher pressure specification in the simulations.

4.3.2 Emergency shutdown - System 2

The emergency shutdown simulation of System 2 was similar to the one of System 1, except for the inclusion of the BOG system and having the pump ESD valve downstream the pump instead of upstream. The additional shutdown activities was thus the closing of the BOG inlet valve (ESD valve) and the shutdown of the compressor. The compressor shutdown was linearly ramped over three seconds since it had no inertia specified and therefor could not produce a realistic shutdown by itself. Also, since the System 2 pump was on the other side of the pump ESD valve compared to System 1, the HP feed pressure have been included in the pressure chart of Figure 4.8. No pressure spikes were observed during the shutdown, however the pump outlet pressure dropped approximately 5.5 bar in just 0.3 seconds. Just as in System 1, the HP feed pressure specification likely let the pressure escape a little too easy.

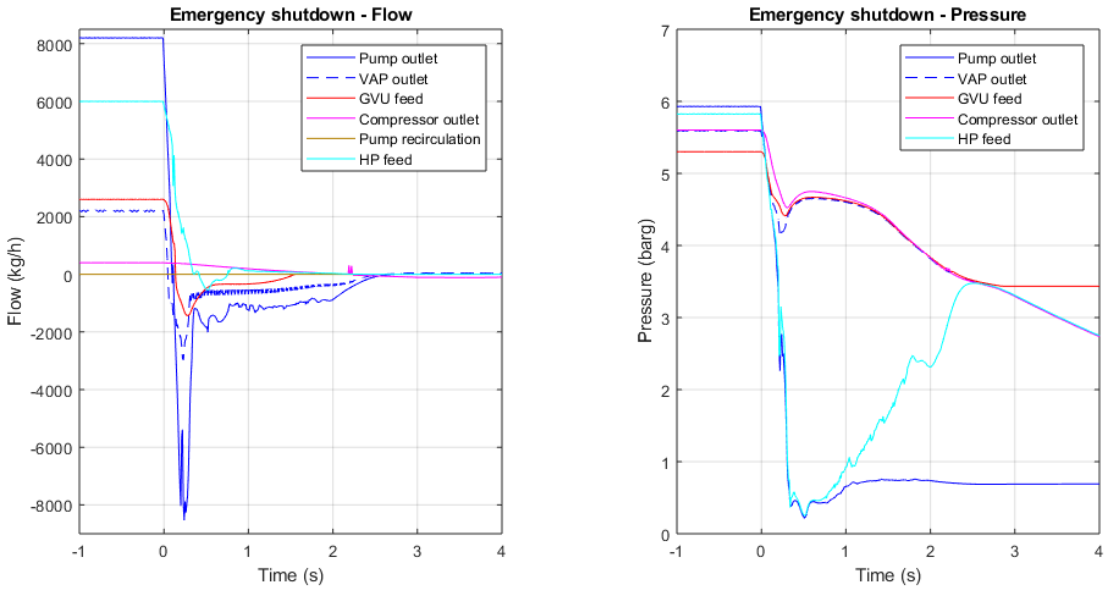

Figure 4.8: Emergency shutdown response of System 2, with mass flows to the left and pressures to the right. The pump recirculation and HP feed has the same pressure.

The overall shape of the curves in Figure 4.8 has some resemblance to the ones of System 1 but are more pronounced. All LNG lines experienced backflow and especially the pump flow was reversed much faster (in 0.2 seconds) and violently compared to System 1 (1 second). This was most likely due to the larger pressure difference of 4.7-0.1=4.6 barg over the system compared to the 4.7-1.99=2.71 barg of System 1, due to System 2 having a near atmospheric LNG tank while System 1 has a pressurized LNG tank.

Through experience with similar pumps, MAN Energy Solutions have approximated emergency pump shutdowns to go from 5800 rpm to zero in 4 seconds and 2000 rpm to zero in 1.5 seconds (Email D. Lindblom, 9 May 2019). An additional shutdown scenario was therefore simulated for System 2, with the approximated emergency shutdown pump speed of 1400 rpm/s as a shutdown speed ramp to result in a longer pump shutdown time. This was the only difference towards the original shutdown simulation and the results are presented in Figure 4.9 and 4.10.

Figure 4.9 shows the pump's linear speed ramp, taking almost twice the time to spin down compared to the other pump shutdowns. Note that the speed drops much lower in System 2 compared to System 1, which is one more indication of the faster backflow to the near-atmospheric pressure tank in System 2.

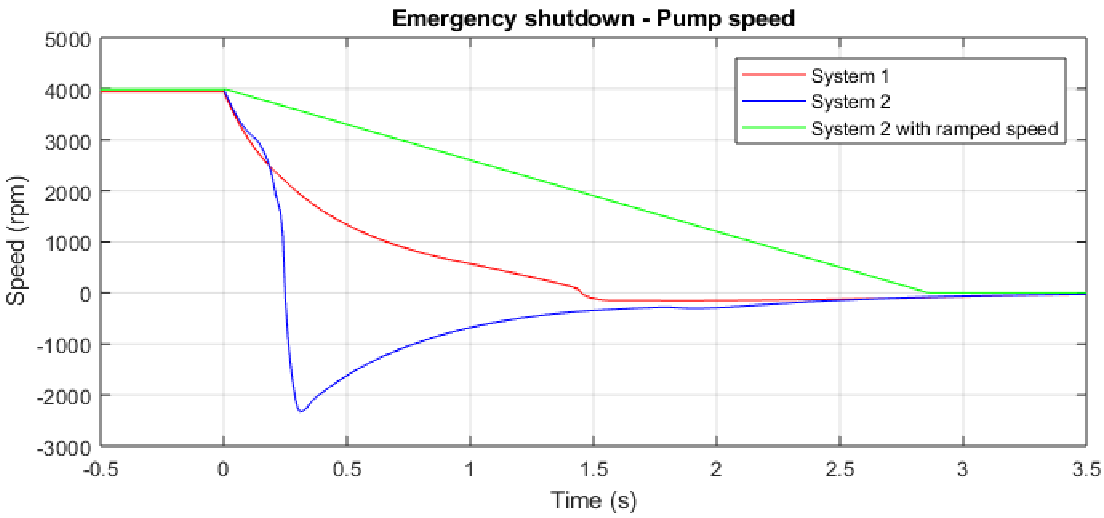

Figure 4.9: Comparison of the pump speeds for the three presented shutdowns: System 1, System 2 and System 2 with ramped speed.

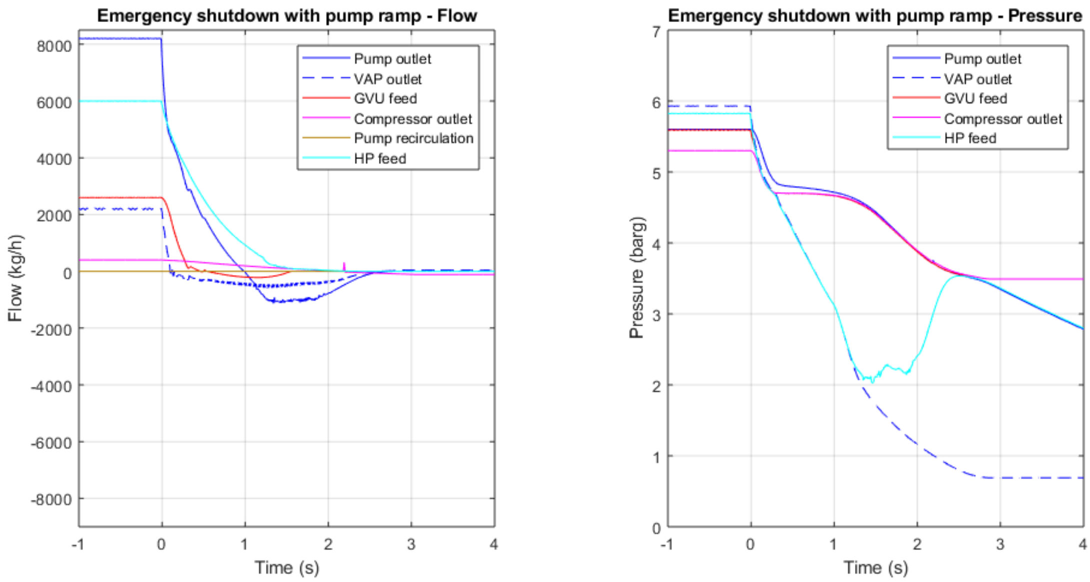

Figure 4.10: Emergency shutdown response of System 2 when using a speed ramp in the pump. To the left are the mass flows of the system and to the right are the corresponding pressures. The axis of the figures are the same as of Figure 4.8 for comparison.

There is much less backflow in the ramped shutdown of Figure 4.10 and the mass flow curves are relatively similar to the shutdown curves of System 1 (Figure 4.7). The slower speed decline of the ramped pump inhibits the pressure to fall as quickly and the backflow of the ramped System 2 (Figure 4.8) is therefor more similar to the shutdown of System 1. Since rotational energy is proportional to the square of rotational speed [46], the speed should have an exponential decrease in case of constant break force. In cases with higher breaking forces, the speed decline would be quicker such as in the original shutdown of System 2. The shutdown mechanics of the pump in System 1 and 2 are thus reasonable, but it could be that the approximated inertias of the pump and electrical motor were too small. This could be one of the reasons of the short spin down times of the original shutdowns compared to the shutdown times of similar pumps experienced by MAN Energy Solutions. The simulated pump had more than double the capacity of the experienced pumps and therefore probably had larger inertia rather than smaller, indicating that the approximated inertia was too small.

4.4 Compressor startup

The membrane storage tank is designed to stay cool but perfect insulation against heating is not always possible. Heat flux from the surroundings enters the cryogenic tank during storage and transportation causing the LNG to evaporate and produce BOG, leading to a pressure increase in the tank. Over short periods of time, the tank can manage this pressure rise but in situations where the pressure increase is prolonged an alternative solution needs to be implemented.

For this process, the BOG was preheated to 0°C after which it was compressed. The BOG heater is used to increase the BOG temperature and thereby avoid high cost of a cryogenic compressor. The compressed BOG was then cooled and fed to the consumers, a simple flow of the BOG is shown in figure 4.11.

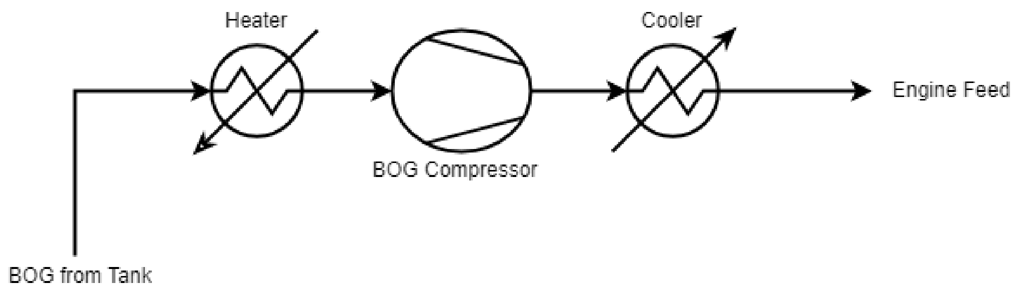

Figure 4.11: Compressor solution for tank pressure reduction.

The aim of the high tank pressure scenario is to examine the disturbance on the GVU feed from starting the compressor. The compressor will deliver around 400 kg/h BOG, which is about 15% the size of the total GVU feed. If the pump's reaction to this new flow is too slow, the engines will be interfered.

The outset of the compressor startup simulation had the pump delivering 6000 kg/h LNG to the HP feed and 2600 kg/h GNG feed to the engines. The HP feed valve, the GVU-valve and the pump were all in AUTO control mode, the compressor was off and the compressor outlet was closed. All inlets had high pressure, which in the membrane tank means 0.7 barg for the BOG and 1.29 barg for the pump inlet due to the LNG's hydrostatic pressure (see Appendix A for the hydrostatic pressure calculation). The scenario then started with the compressor ramping up during 2.5 seconds to 900 rpm, a speed which produces 400 kg/h BOG at high tank pressure. During this ramp, as the compressor outlet pressure reaches slight overpressure (0.1 barg) against the GNG connection, the compressor outlet valve was opened. The system's reaction to the additional BOG flow is presented in Figure 4.12.

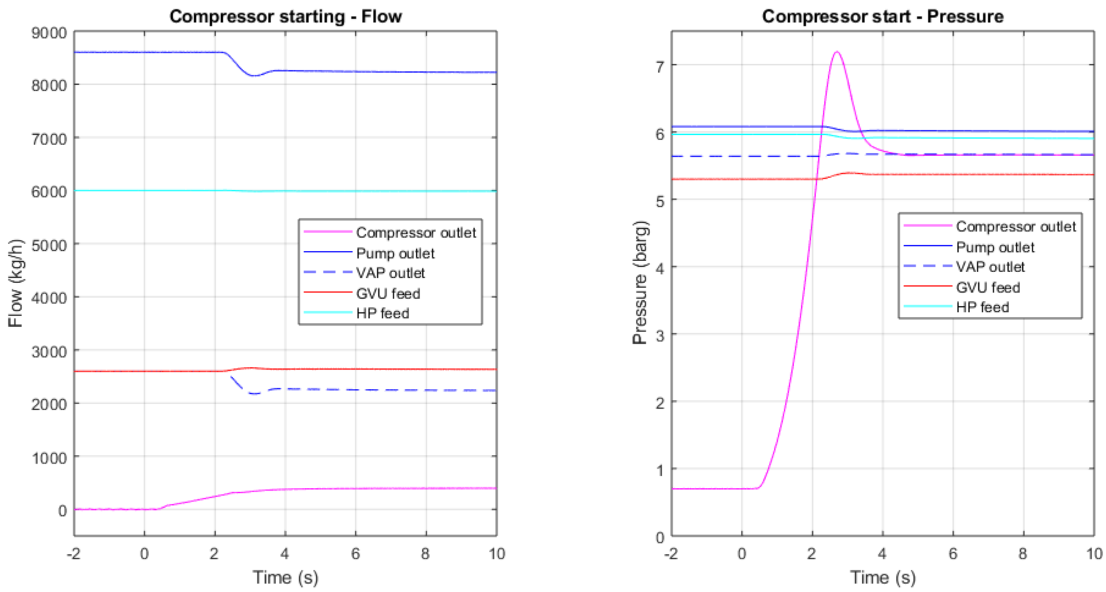

Figure 4.12: Flows (left) and pressures (right) during the compressor startup.

In Figure 4.12 it can be seen that the change to the LNG line occured over 1.5 seconds and that the HP feed was more or less unaffected. The disturbance to the GVU feed appears to have been of minor proportions, however, the engine manual expresses that any pressure gradients above 0.1 bar/s and any pressure peaks above 0.5 bar will lead to disturbances in the engine. During the third second, the pressure gradient in the GVU feed reached 0.1015 bar/s, which may just have been enough to cause engine disruptions.

4.4.1 Compressor start with feedforward control

The feedforward controller was tested on the compressor start scenario, where it produced a slightly higher pressure gradient in the GVU feed (0.1085 bar/s) compared to the original system (0.1015 bar/s). However, as can be seen in Figure 4.13, the dot-dashed lines of the feedforward system went down to the new steady state in three seconds (from second two to five), which was much faster than the original system (filled lines) which had a slow decline of approximately 80 seconds. The indication is thus that feedforward hastens the pump response to compressor changes, both increasing the pressure gradient and the rate of which the system returns to steady state.

4.4.2 Compressor startup with buffer vessel

The compressor start scenario was also tested with the 2m^3 buffer equipped system. The results are shown in Figure 4.14, where the filled lines represent the original system and dashed curves represent the buffer equipped system. In both simulations, the compressor pressure turned downwards as the compressor outlet was opened and during this time (approximately second two to four) the GVU feed experienced a pressure change. It can be seen in Figure 4.14 that the dashed lines of the buffer equipped system were a bit smoother than the filled lines, which just had higher than allowed pressure gradient. The buffer vessel brought down the GVU pressure gradient to 0.071 bar/s which was low enough to avoid engine disturbance.

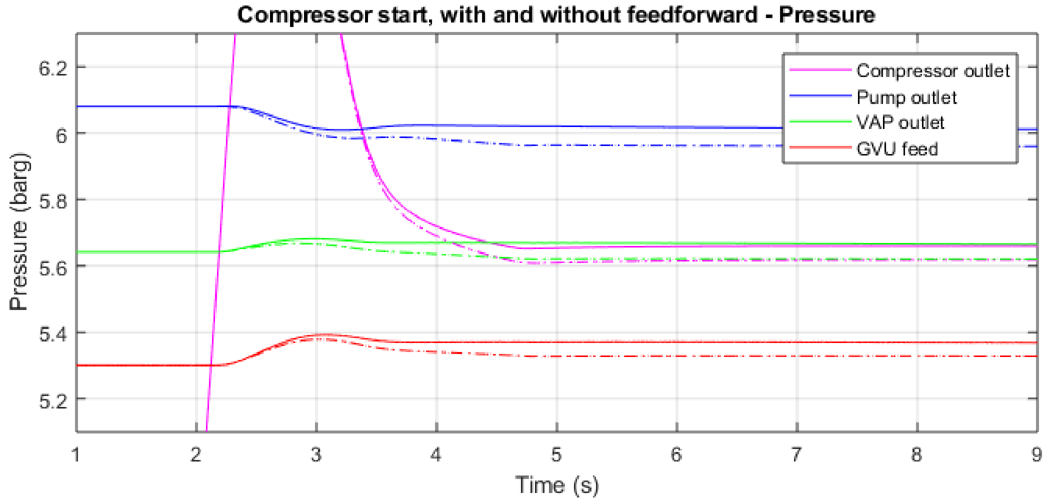

Figure 4.13: Comparison of the pressures during compressor startup, when having feedforward or not. Filled lines are the original system and dot-dashed lines are with feedforward control.

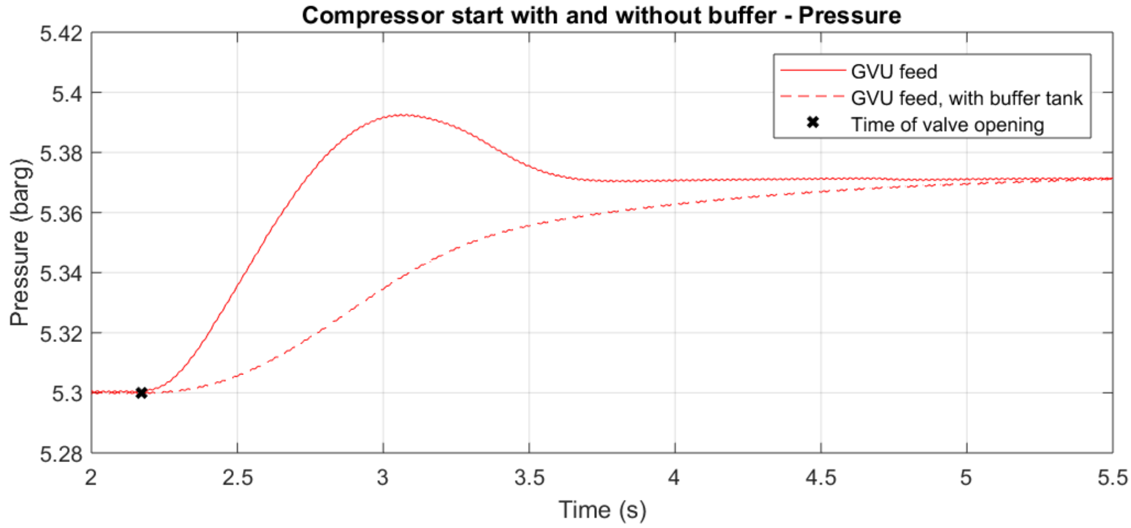

Figure 4.14: Comparison of the system pressures during compressor startup when equipped buffer or not. Filled lines are without buffer and dashed line are with buffer.

Because the buffer vessel mitigated the pressure disturbance of the compressor startup but slowed down the system control, the feedforward control was also included in some buffer vessel simulations to increase the reactivity of the pump control towards the compressor. This was done with two levels of feedforward control, K_p=-0.035 and K_p=-0.07, and the result on the GVU pressure can be seen in Figure 4.15.

In this case, more aggressive feedforward control produced lower pressure gradient but it also undershot the steady state pressure of 5.3 bar slightly. The two feedforward controllers reached the steady state pressure around the same time, several minutes before the system without feedforward control.

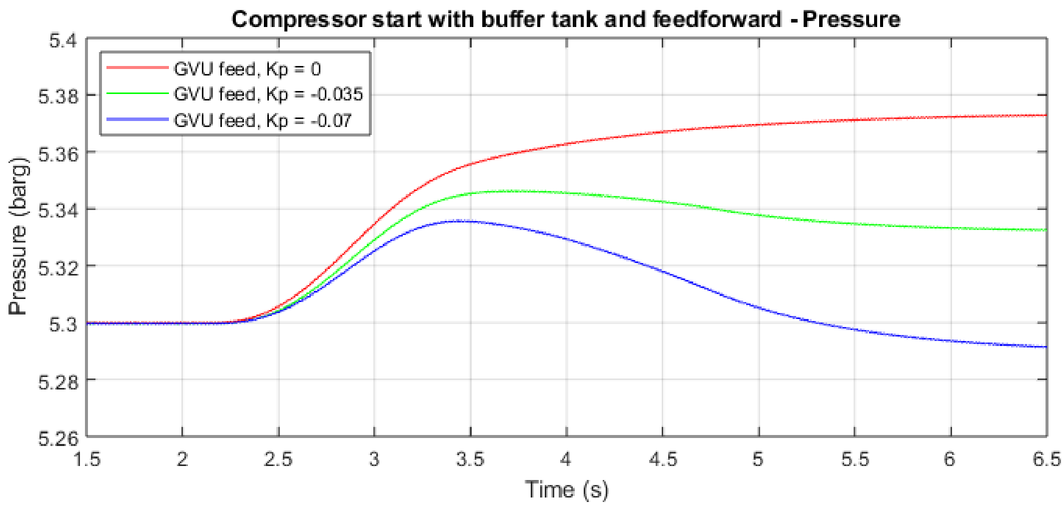

Figure 4.15: Comparison of the system pressures when having buffer and using varying degrees of compressor speed feedforward to the pump. The red line ha no feedforward effect.

4.5 Low tank pressure

In this scenario, the effects of low tank pressure on the performance of the standalone pump and the overall process were investigated, keeping in mind that the recommended operating tank pressures are as given in 4.2. The effects of low tank pressure were not studied for the membrane tank in System 2 since the pump is submerged into the tank. It therefor lacks the pipe and valve before the pump which gives it higher available NPSH at the pump inlet and less risk of cavitation.

Table 4.2: Recommended Operating Pressures

Pressure	bar
$P_{recommended,min}$	3
$P_{recommended}$	5
$P_{recommended,max}$	7.5

Bunkering and sloshing are the main processes that cause pressure changes in storage tanks. The bunkering of LNG into the tank can be done from the top or the bottom of the tank, the selection of the bunkering method used depends largely on the pressure inside the tank. In a situation where the tank pressure is higher than the saturation pressure of the LNG being bunkered, the LNG is fed from the top which in turn leads to a pressure drop. Sloshing on the other hand usually occurs on rapid unstable waters and causes condensation of gaseous natural gas. The effect of this is a drop in the tank pressure.

To study the effects of the low tank pressure, the process was run until stable, after which the pump inlet pressure was reduced by 0.5 bar intervals until the system failed to converge. The step changes were made to help determine the exact pressure that would have a large effect on the process. The result of these changes can be seen in Figure 4.16. Figure 4.16 shows the relationship between the main operating streams (flows and pressures) and pump speed. As the inlet pressure was dropped, the system managed to stay stable for 5 seconds, after which the pump outlet flow spiked to about 9000 kg/h. This spike was caused by a spike in the pump speed as it tried to attain the required operating pressure. After 5 seconds, the feed pressure was set to 0.3 barg which led to severe pump cavitation and flow reversal. The subsequent pressure drop led to a pump speed increase, without effect to the flow. The reversed GVU flow is of the pressure 4.7 barg due to the pressure specification of the GVU-outlet, which is the origin of the simulation's reversed flow.

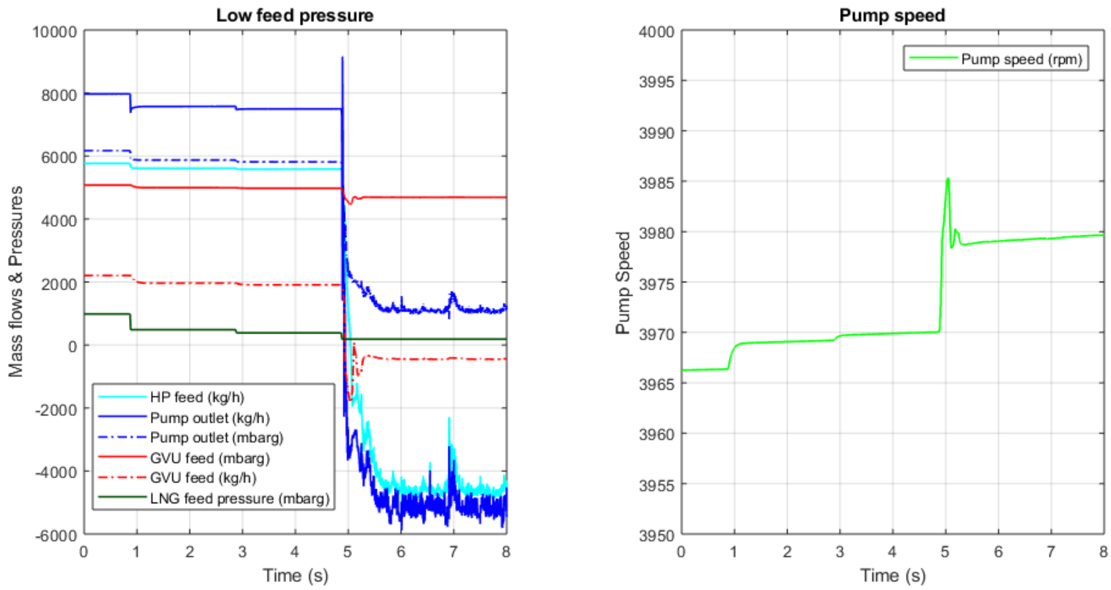

Figure 4.16: System behavior when the feed passes the low pressure mark. To the left are pressures and mass flows while to the right is the pump speed.

The pressure of the tank should be the lowest just after bunkering, when the hydrostatic pressure is at its maximum (between 0.1 and 0.3 bar depending on tank size and liquid level). Since the operational pressure of the vacuum insulated LNG tank ranges between 2 and 6.5 barg plus the hydrostatic pressure at full tank (0.15-0.3 bar), the development of such a low pressure is not probable.

4.6 GVU pipe length comparison

The effect of placing the controller within the FGSS (upstream the master valve) was also studied. The reason behind this study was to determine whether the length of the gas pipe had an effect of how fast the controller implements the changes in the system when the controller was not placed at the GVU. During the study, two systems with 15 m DN80 pipe respectively 150 m DN100 pipe were ramped from 650 kg/h load to 1300 kg/h within 60 seconds (the flow and time of two engines from loading up from 50% to 100%, according to the engine manual). The results from this run, which were very similar, can be seen in Figure 4.17.

Further analysis of the results as seen in Figure 4.18 showed that there was very little difference between both pipes. The 150m pipe curves are a bit rounder due to the larger buffer volume, but the shapes of the curves are in large very similar. Hence one can conclude that the pipe length has no notable effect on the controllers response time within the 150 m range.

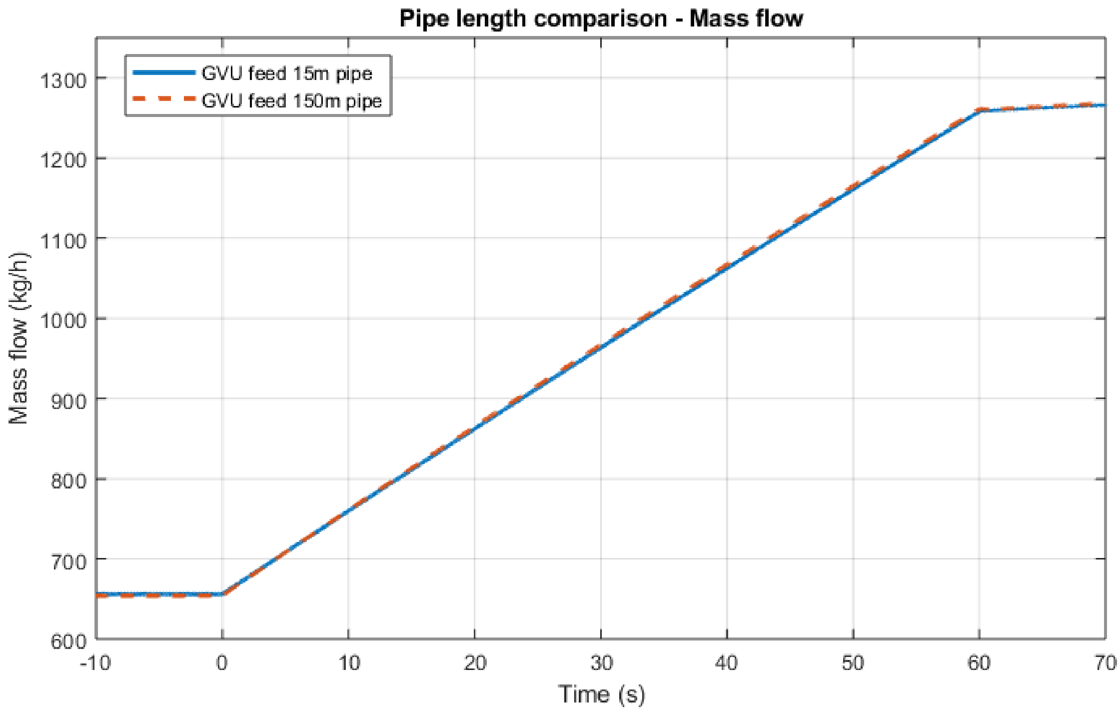

Figure 4.17: Flows to GVU for 15m and 150m pipes during the 60 second acceleration of two engines from 50% load to 100% load.

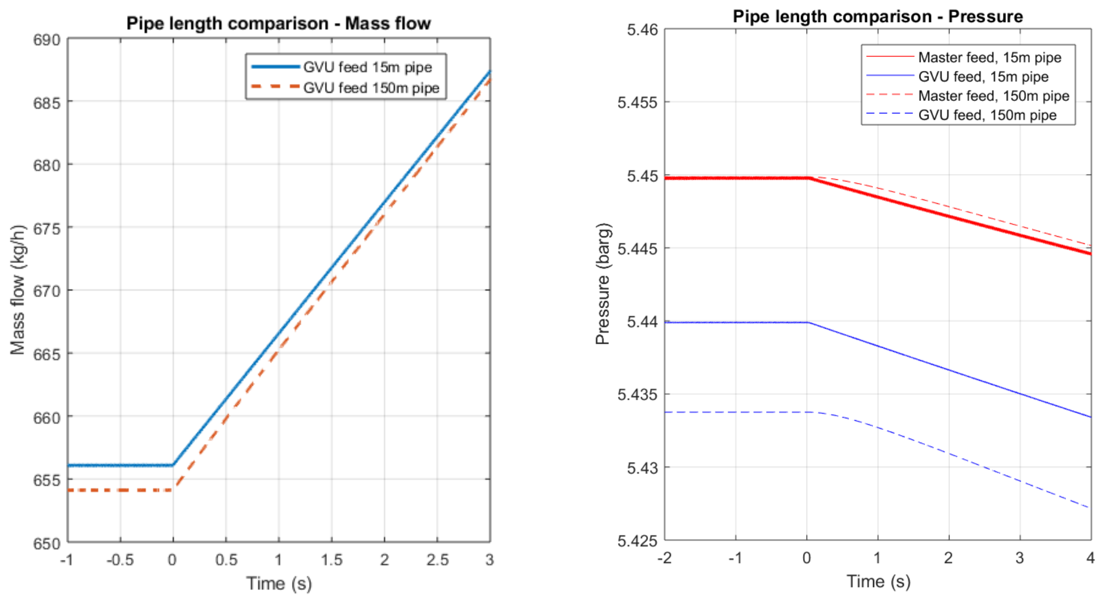

Figure 4.18: Comparison between the mass flows and pressures produced from using 15m and 150m pipes.

5. Conclusion

The automatic control of the process was evaluated based on the scenarios with automatic control, i.e. the loadup and compressor start scenarios. In the simulations, the pump, compressor, HP feed valve and GVU valves all used automatic controls at some point.

Feedback control was implemented in both systems' pumps, where it effectively controlled the operating pressure between the master valve and the GVU. Its effect can be seen in the loadup, compressor startup and low-pressure scenarios (Chapters 4.2, 4.4 and 4.5 respectively). The feedback control could be tuned better however, since it takes a long time to erase the last few percentage of error, which can be seen in Figures 4.3, 4.5, 4.13, 4.15 and 4.16 together with the explanatory text around them. Also, it was found that the pressure feedback for the pump can be collected upstream the master valve instead of at the GVU.

The automatic pressure feedback control of the compressor was not simulated in this study, but it was manually controlled similarly to an on/off controller. The drastic change induced by this control just barely caused disturbances in the original system's GVU feed. A mild tank pressure PI control should therefore be possible to use without introducing any instabilities to the system. If using a buffer tank, the on/off control should not be a problem to the GVU feed.

One variable not covered in this work of simulation was the control of the minimum flow line. This line needs to be used at low loads when the minimum speed of the pump delivers too much fuel to the GVU and have to be inefficiently throttled. The control of the minimum flow line would need to be well thought out, since it has to function properly at low pump speeds but not recirculate LNG in vain. Recirculated LNG is slightly heated and will contribute to increased boil off and faster pressure rise in the storage tank.

During emergency shutdown of both systems no pressure spikes were observed. However, in the case of System 2, the pump experienced a rapid and large backflow. Simulations have shown that a longer rundown time of the pump would decrease this backflow significantly and the rapid backflow might have been due to the uncertain estimation of pump inertia. Also, to produce a more realistic shutdown scenario, the HP feed could be developed further to resemble the real system more in pressures and holdup volume.

The need of additional buffer volume in the process was also investigated. The addition of a $2m^3$ buffer vessel before the master valve helped keep System 2 stable during compressor disturbances but slowed down the control of the system. The stabilizing effect was further enhanced when the buffer vessel was combined with feedforward control. The effect of the buffer vessel was less apparent in System 1 and 2 during engine and pump flow changes. The final conclusion was that the buffer vessel will not be a necessity to avoid engine disturbances, if the control is automatic and well tuned.

Lastly, the lower feed pressure limit of System 1 was found at 0.3 barg. This is very low and considering the operational pressure of the vacuum insulated tank plus the liquid's hydrostatic pressure, such a pressure is not likely to arise.

5.1 Areas of future improvement

There are some elements that can be adjusted to enhance the accuracy of the simulation. The compressor needs performance curves and inertias to be modeled properly, as well as a designated computational block for rotary vane compressors. Two of the system's boundary conditions, the GVU but especially HP feed could be investigated further. Lastly, the pump has some uncertainty regarding inertia which could be resolved by dialogue with the manufacturer.

Bibliography

[1] International Maritime Organization.Studies on the Feasibility and use of LNG as a Fuel for Shipping.4 Albert Embankment, London SE1 7SR. IMO; 2016

[2] DieselNet.IMO Marine Engine Regulations [Internet]. ECOpoint Inc. 2018 [Aug 2018; 24 Jan 2019] Available from: www.dieselnet.com/standards/inter/imo.php

[3] MarineInsight[Internet]. Hapaq-Lloyd; 2016 [cited 2019 Jan 24]. Available from: www.marineinsight.com/shipping-news/how-the-new-fuel-regulations-change-the-entire-shipping-industry/

[4] Brown J. Alternative fuels: The future of zero emissions shipping [Internet]. Environmental Defense Fund; 2018 [cited 2019 Feb 14] Available from: www.europe.edf.org/news/2018/31/07/alternative-fuels-future-zero-emissions-shipping

[5] Lloyd's Register and UMAS. Zero-emission vessels 2030. How do we get there? [Internet]. Lloyds Register Group Limited; 2017 [cited 2019 Feb 14] Available from: www.lrs.or.jp/news/pdf/LR_Zero_Emission_Vessels_2030.pdf

[6] Sames PC, Clausen NB and Andersen ML, editors. Cost and Benefits of LNG as Ship Fuel for Container Vessels. MAN Diesel & Turbo, 2011.

[7] Xu S, Cheng Q, Zhuang L, Tang B, Ren Q and Zhang X. LNG vaporizers using various refrigerants as intermediate fluid: Comparison of the required heat transfer area. J Nat Gas Sci Eng. 2015 July; 25:(1-9). DOI: doi.org/10.1016/j.jngse.2015.04.031

[8] World Ports Climate Initiative. What is LNG? [Internet]. World Ports Climate Initiative; [cited 2019 Jan 25]. Available from: www.lngbunkering.org/lng/LNG

[9] MAN Energy Solutions. LNG Fuel Gas Systems [Internet]. MAN Energy Solutions; [cited 2019 Jan 25]. Available from: www.marine.man-es.com/technology/marine-fuel-gas-systems/lng-fuel-gas-systems

[10] Chorowshi M, Duda P, Polinski J and Skrzypacz J. LNG systems for natural gas propelled ships. IOP Conf Ser Mater Sci Eng. 2015;101.

[11] Marine Service Noord. Three Design Concepts For Lng Fuel Systems [Internet]. Marine Service Noord; [cited 2019 Jan 25]. Available from: www.marine-service-noord.com/three-design-concepts-for-lng-fuel-systems/

[12] Rachow M, Loest S and Sitinjak LRM. Concept for a LNG Gas Handling System for a Dual Fuel Engine. Int J Mar Eng Innov Res. 2017 Sep;1(4):272-283.

[13] Michael Smith Engineers ltd. Useful information on centrifugal pumps [Internet]. Michael Smith Engineers Publisher; 2019 [Cited 2019 March 19]. Available from:

www.michael-smith-engineers.co.uk/resources/useful-info/centrifugal-pumps

[14] The Centrifugal Pump [Internet]. [Cited 2019 March 19]. Available from: https://us.grundfos.com/content/dam/Global%20Site/Industries%20&%20solutions/Industry/pdf/The_Centrifugal_Pump.pdf

[15] Mechanical Engineering Site. How to Read a Centrifugal Pump Performance Curve. 2018 May 3 [Cited 2019 March 20]. In: Mechanical Engineering Site [Blog on the Internet]. 2017- . Available from: www.mechanicalengineeringsite.com/how-to-read-a-centrifugal-pump-performance-curve/

[16] CASCO USA. Positive Displacement Compressors [Internet]. 2014 [Cited 2019 March 13] Available from: www.cascousa.com/compressed-air-101/types-of-compressors/positive-displacement-compressors/

[17] GANZAIR. Rotary Vane Compressors for Vehicle Applications [Internet]. Kiskunhalas, Hungary: Ganzair Compressor Technologies Ltd.; [Cited 2019 March 13]. Available from: www.rustrade.hu/07_Kommercheskie_predlojenia_i_zaprosi/07_03_Predlojenia_veng_export/07_03_01_Tovar/07_03_01_16%%20Tovari/ROTRY%20VANE%20COMPRESSORS%20FOR%20VEHICLE%20APPLICATIONS%20V1.0.pdf

[18] Belting-Clar C and Bleicher L. Quench the flare [Internet]. Farnham: Palladian Publications Ltd; 2017 [Cited 2019 March 14]. Available from: www.lngindustry.com/special-reports/07032017/quench-the-flare/

[19] Azih C. Experimental and Theoretical Investigation of a Sliding Vane Compressor-Expander Unit for an R-134a Automotive Vapour Compression Refrigeration System. Ottawa: Carleton University; 2007.

[20] Davey Compressor Company. Different Type Air Compressors [Internet]. Somerset: Davey Compressor Company; 2003 [Cited 2019 March 14]. Available from: www.daveycompressor.com/differenttype.html

[21] LNG storage tank.[Updated 2018 April 03; cited 2019 March 13]. Available from: https://en.wikipedia.org/wiki/LNG_storage_tank

[22] Karlsson S. Creating Optimal LNG Storage Solutions [Internet]. Helsinki: In detail magazine; 2015 [Cited 2019 March 14]. Available from: www.wartsila.com/twentyfour7/in-detail/creating-optimal-lng-storage-solutions

[23] Saeid M and John Y. M and Jaleel V. V and David A. W. Handbook of Liquefied Natural Gas. Boston: Gulf Professional Publishing; 2014

[24] Hussain YA. Heat Exchangers [degree project/master's thesis on the Internet]. Jordan University of Science and Technology; [Cited 2019 March 18]. Available from: http://www.just.edu.jo/ yahussain/files/Heat%20Exchangers.pdf

[25] John Hellborg. Modelling of shell and tube heat exchangers [master's thesis on the Internet]. Lund University; 2017 [2019 April 17]. Available from: http://lup.lub.lu.se/luur/download?func=downloadFile&recordOId=8900243&fileOId=8900249

[26] Skousen P.L. Valve Handbook. 3 ed. New York: McGraw-Hill; 2011. ISBN: 9780071743891

[27] Flowserve. Performance! 12.0 User Guide - Flow Characteristics [Internet]. Irving, Texas: Flowserve Corporation; date unknown [Updated 2013, cited 2019 March 19]. Available from: http://www.flowserveperformance.com/performhelp/sizing_selection:valtek:flow_characteristics

[28] PIPE FLOW fluid thinking software solutions. Pipe Pressure Drop Calculations [Internet]. PIPE FLOW fluid thinking software solutions; 2019 [updated:2019 March 18; cited: 2019 March 18]. Available from: www.pipeflow.com/pipe-pressure-drop-calculations

[29] IHS Harmony Reference Materials. Pressure loss calculations [Internet]. London: IHS Inc.; 2017 [Updated 2017 November 30, cited 2019 March 20]. Available from: www.ihsenergy.ca/support/documentation_ca/Harmony/content/html_files/reference_material/calculations_and_correlations/pressure_loss_calculations.htm

[30] AspenTech. Aspen HYSYS Help, V10 [computer program]. Bedford (MA): Aspen Technology Inc; 2017 [cited 1 March 2019].

[31] Neutrium. Speed of sound in fluids and fluid in pipes [Internet]. Native Dynamics; 2014 [Cited 2019 March 20]. Available from: https://neutrium.net/fluid_flow/speed-of-sound-in-fluids-and-fluid-in-pipes/

[32] Bernasconi G, Del Guidice S, Giunta G, Dionigi F, Schiavon R, Zanon F. Advanced pipeline monitoring using multipoint acoustic data. Offshore Mediterranean Conference and Exhibition. 2013, Ravenna, Italy: 2013.
DOI: https://doi.org/10.13140/RG.2.1.4233.5767

[33] Meng Y, Li H, Li G, Zhu L, Wei N, Lin N. Investigation on propagation characteristics of the pressure wave in gas flow through pipes and its application in gas drilling. J. Nat. Gas. Scs. Eng. 2015; 22: pages 163:171.
DOI: https://doi.org/10.1016/j.jngse.2014.11.026

[34] Faanes A. and Skogestad S. Buffer tank design for acceptable control performance. Ind. Eng. Chem. Res. 2003; 42(10):2198-2208.

[35] Grundfos Encyclopedia. Buffer tank [Internet]. Bjerringbro, Denmark: Grundfos; 2015 [Cited 2019 March 15]. Available from:
https://www.grundfos.com/service-support/encyclopedia-search/buffer-tank.html

[36] Cheng B. Review of turbulent mixing models. Acta Math Sci. 2009; 19(6): 1703-1710.
DOI: doi.org/10.1016/S0252-9602(10)60012-4

[37] Marlin T.E. Process Control - Designing Processes and Control Systems for Dynamic Performance. 2 ed. Hamilton, Canada: McMaster University; 2015 [Cited 2019 March 29]. Available from: http://pc-textbook.mcmaster.ca/Marlin-Ch01.pdf

[38] Corriou JP. Process control - Theory and applications. 2 ed. Cham, Switzerland: Springer International Publishing AG. DOI: doi.org/10.1007/978-3-319-61143-3

[39] Åström KJ. Control system sesign lecture notes for ME 155A [Internet]. Santa Barbara, USA: University of California; 2002 [Cited 2019 May 3]. Available from:http://www.cds.caltech.edu/ murray/amwiki/index.php?title=Main_Page

[40] Dixon P. The velocity of PID [Internet]. Control engineering; 2016 [Cited 2019 May 3]. Available from : www.controleng.com/articles/the-velocity-of-pid/

[41] Smuts J. A tutorial on feedforward control [Internet]. Opticontrols; 2011 [Cited 2019 May 9]. Available from: http://blog.opticontrols.com/archives/297

[42] Smuts J. A tutorial on cascade control [Internet]. Opticontrols; 2010 [Cited 2019 May 3]. Available from: http://blog.opticontrols.com/archives/105

[43] Lopez-Echeverry JS, Reif-Acherman S, Araujo-Lopez E. Peng-Robinson equation of state: 40 years through cubics. Fluid Ph. Equilibria. 2017 Sep; 447: 39-71. DOI: https://doi.org/10.1016/j.fluid.2017.05.007

[44] Carlson EC. Don't Gamble With Physical Properties For Simulations. Chem. Eng. Prog. 1996; 92(10): 35-46.

[45] Annex 11 - Interim Guidelines on Safety for Natural Gas-Fuelled Engine Installations in Ships (Resolution MSC.285(86): 2009). London: International Maritime Organization.

[46] Hyperphysics. Rotational Kinetic Energy [Internet]. Atlanda, USA: Georgia State University; 2000 [Updated 2004, cited 15 May 2019]. Available from: http://hyperphysics.phy-astr.gsu.edu/hbase/rke.html

A. Appendix

A.1 Pump specifications

The motor's synchronous speed is calculated by the electrical frequency and the number of poles in the motor as: synchronous speed = 120 · 50Hz / 2poles = 3000rpm. Gear ratio was calculated as 6000rpm / 2900rpm = 2.07. The typical operating capacity was specified as the rated capacity which is 17 m^3/h. The figures used to estimate the pump and motor inertias are presented in Table A.1 below.

Table A.1: Design power and speed for the inertias of the pump and electrical motor. *Rounded value of 95-98% range of the motor's synchronous speed.

	Pump	Electrical motor
Power (kW)	6.08	16
Speed (rpm/1000)	6	2.9*

A.2 Pump curve information

Table A.2: Data used to develop the curves for the centrifugal pump used. The far left column shows the rotational speed of the pump in rpm.

4000	Flow	0.0	5.80	9.70	15.50	19.40	23.30
	Head	151	151	150	136	119	96
	Efficiency %	0.0	41.10	55.10	67.50	70	68
4300	Flow	0.0	6.30	10.40	16.70	20.80	25.0
	Head	175	175	173	158	138	111
	Efficiency %	0.0	41.10	55.10	67.50	70.0	68.0
4400	Flow	0.0	6.40	10.70	17.10	21.30	25.60
	Head	183	183	182	165	144	116
	Efficiency %	0.0	41.1	55.10	67.50	70	68
4700	Flow	0.00	6.80	11.40	18.20	22.80	27.30
	Head	209	209	207	188	165	133
	Efficiency %	0.0	41.10	55.10	67.50	70	68

Table A.3: $NPSH_R$ curves specified to the pump.

Speed (rpm)	$NPSH_R$ (m)	Capacity (m^3/h)
4000	0.26	5.8
	0.18	19.4
4400	0.29	6.4
	0.2	21.3
4700	0.33	6.8
	0.22	22.8

A.3 Hydrostatic tank pressure calculation

The hydrostatic pressure in the membrane storage tank was calculated with the formula $\Delta P_{hs} = \rho g h$, with the LNG density 435kg/m^3, gravitational acceleration 9.81m/s^2 and liquid height 14m. This liquid height account for a liquid level of 83% in the 16.9m high tank, producing 0.59 bar hydrostatic pressure.

The hydrostatic pressure in the vacuum insulated tank depends on the diameter and filling level of the tank. The available vaccum tank diameters varies between 3.6 and 6.9 meter[1], giving the the maximal hydrostatic pressure a range of 0.15 to 0.3 bar.

[1]MAN product specification of vacuum insulated tanks: https://sweden.man-es.com/docs/librariesprovider16/cryo-files/6-2-product-specification-vacuum-insulated-tank.pdf?sfvrsn=bd7fda2_2

B. Appendix

B.1 HYSYS representation of System 1 and 2

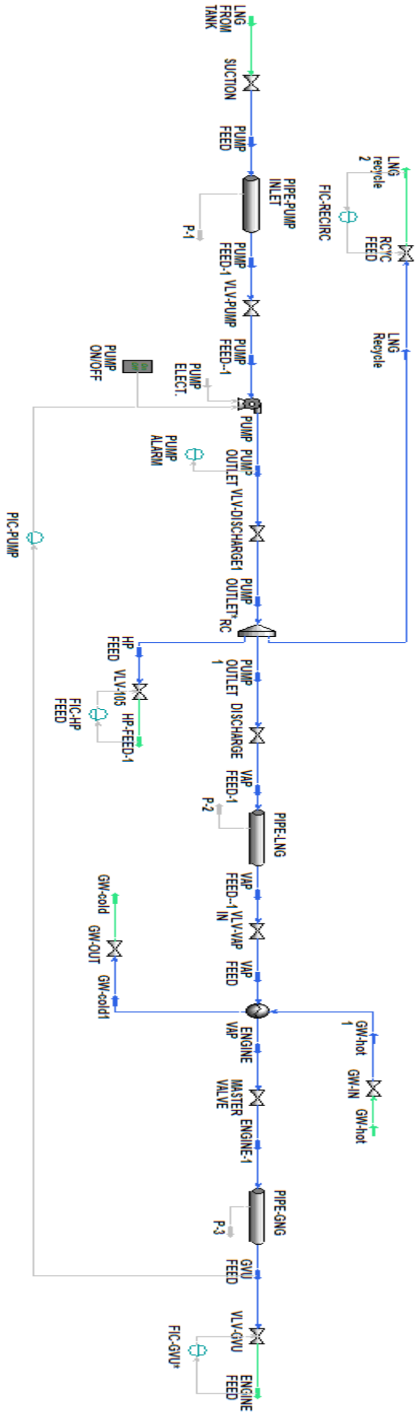

Figure B.1: The simulation flow sheet of System 1.

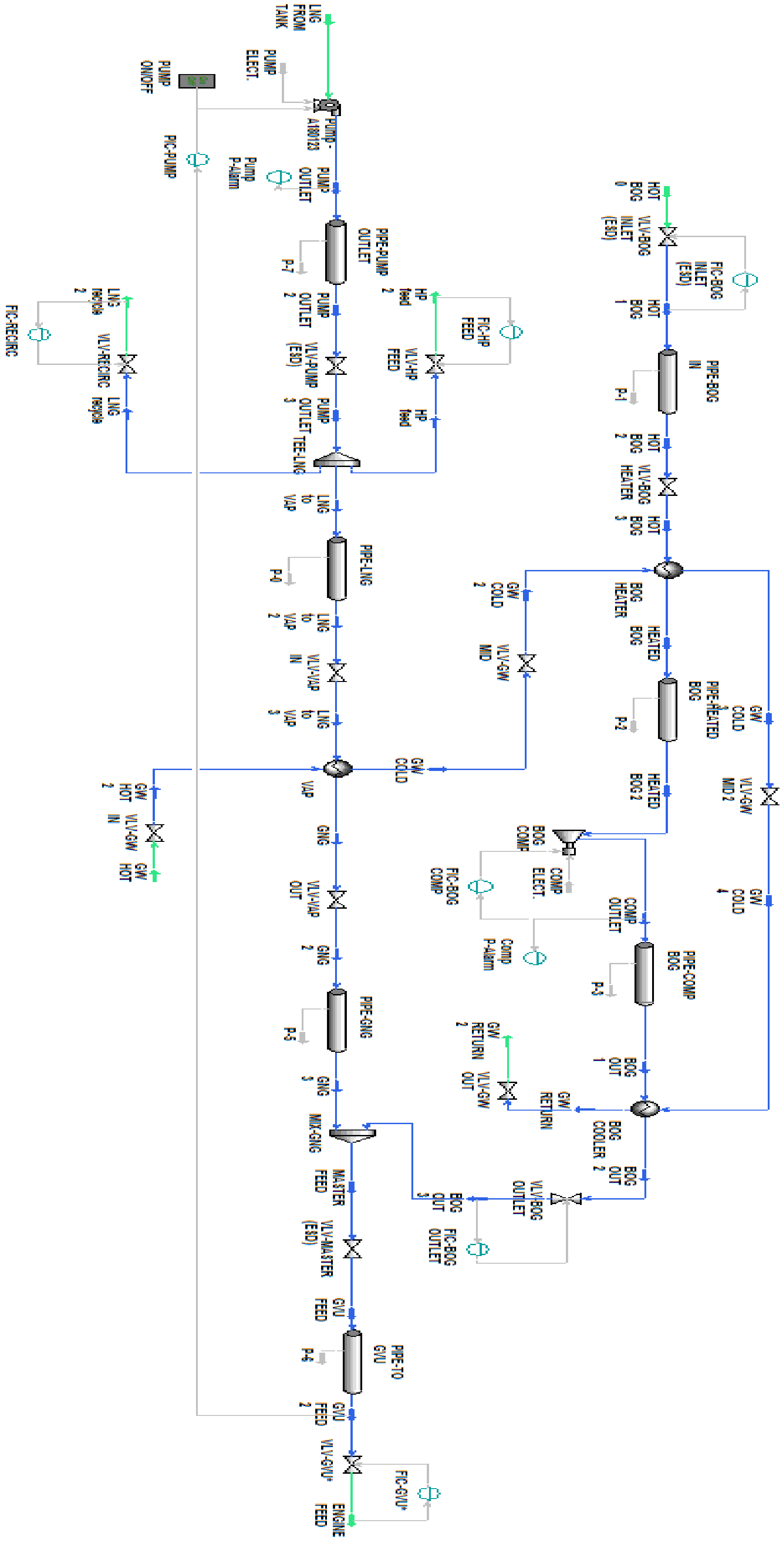

Figure B.2: The simulation flow sheet of System 2.